École Nationale Supèrieure d'Ingénieur de Caen

Intership Report

STABILITY ANALYSIS OF SATURATED DISCRETE-TIME SYSTEMS THROUGH THE USE OF SIGN-INDEFINITE QUADRATIC FORMS

April – August 2025
Toulouse, France

Luana **ALBUQUERQUE**
Academic Year: 2024/2025
GSPE - SATE

Supervisor: Sophie **TARBOURIECH**
Co-supervisor: Olivier **GEHAN**

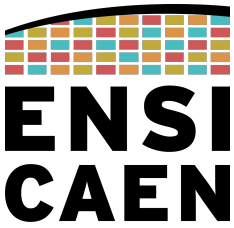

LAAS-CNRS

The LAAS-CNRS (Laboratory for Analysis and Architecture of Systems), located in Toulouse, France, is one of the most prominent research centers in Europe. Known for its interdisciplinary approach, the lab conducts advanced research in areas such as robotics, control systems, and biotechnology. It maintains active partnerships with major industrial players, including Airbus and Thales. Research groups like Gepetto, internationally recognized for their work in humanoid robotics and motion control, underscore LAAS's leading role in the development of autonomous systems.

In the field of control, the MAC team (Méthodes et Algorithmes en Commande) stands out for its research on systems with constraints, nonlinearities, and actuator saturation. The team develops state-of-the-art control methods based on Lyapunov functions, Linear Matrix Inequalities (LMIs), and convex optimization, with practical applications in aerospace, smart grids, autonomous vehicles, and embedded systems. With numerous scientific publications and involvement in collaborative research projects, MAC is regarded as a global reference in advanced control techniques.

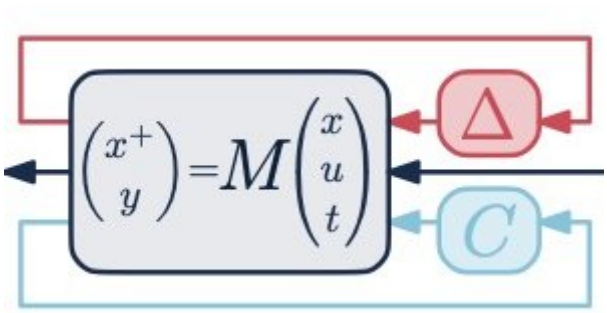

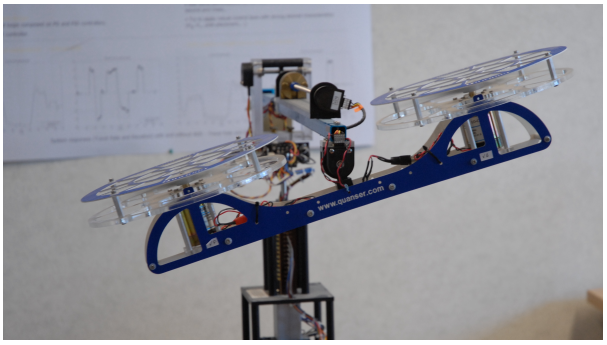

Figure 1: MAC team at LAAS-CNRS (Toulouse, France)

Watch the lab's promotional video:

Abstract

Every physical device is subject to operational limitations, and a common strategy to address this issue is to oversize the actuators so that their operating range fully encompasses the system's requirements. However, this approach is often impractical due to constraints such as cost, space, or energy efficiency. In such cases, actuator saturation becomes unavoidable, introducing a highly nonlinear behavior into the system.

This nonlinearity compromises the validity of classical control techniques based on local linearization and frequency-domain analysis. To handle this scenario, Lyapunov functions provide a robust alternative for stability analysis, as they allow the direct consideration of saturation effects and the system's global nonlinear dynamics.

This work focuses on the stability analysis of discrete-time systems with input saturation. We propose a new formulation of Lyapunov stability conditions that allows the use of sign-indefinite matrices in the Lyapunov function. By applying the S-procedure, this method enables the verification of asymptotic stability while offering additional degrees of freedom in the modeling process.

The proposed approach is inspired by the continuous-time study presented in [1] and is adapted here to the discrete-time case. The same framework is preserved, addressing four cases: analysis and control synthesis, both in global and regional settings.

Keywords: Nonlinear systems, Lyapunov stability, sign-indefinite matrix, saturation.

Résumé

Tout dispositif physique est soumis à des limitations opérationnelles. Une stratégie courante pour contourner ce problème consiste à surdimensionner les actionneurs afin que leur plage de fonctionnement couvre entièrement les exigences du système. Toutefois, cette approche s'avère souvent impraticable en raison de contraintes liées au coût, à l'espace ou à l'efficacité énergétique. Dans ces cas, la saturation des actionneurs devient inévitable, introduisant un comportement fortement non linéaire dans le système.

Cette non-linéarité compromet la validité des techniques de commande classiques basées sur la linéarisation locale et l'analyse fréquentielle. Pour traiter cette situation, les fonctions de Lyapunov offrent une alternative robuste pour l'analyse de stabilité, car elles permettent de prendre directement en compte les effets de saturation ainsi que la dynamique non linéaire globale du système.

Ce travail porte sur l'analyse de la stabilité des systèmes à temps discret avec saturation en entrée. Nous proposons une nouvelle formulation des conditions de stabilité de Lyapunov autorisant l'utilisation de matrices non définies positives dans la fonction de Lyapunov. En appliquant la procédure S, cette méthode permet de vérifier la stabilité asymptotique tout en offrant des degrés de liberté supplémentaires dans la modélisation.

L'approche proposée s'inspire de l'étude en temps continu présentée dans [1] et est ici adaptée au cas en temps discret. Le cadre théorique est conservé, en abordant les quatre cas suivants : analyse et synthèse de commande, à la fois dans un cadre global et régional.

Mots-clés: Systèmes non linéaires, stabilité de Lyapunov, matrice non définie positive, saturation.

Contents

1 Introduction

This work was structured to provide the theoretical foundation required to understand the stability analysis of discrete-time systems with saturation, based on the use of indefinite-sign quadratic Lyapunov functions. The introduction addresses the relevance of saturation in control systems, the role of anti-windup techniques in handling this nonlinearity, and the fundamental concepts and notations used throughout the study. Then, in Section 2, the saturation and dead-zone functions are modeled along with the system formulation, and the sector condition is introduced, which serves as the theoretical basis for the developments that follow.

Following this, Section 3 presents the Lyapunov LMIs and the stability conditions for both controller synthesis and stability analysis, in global and regional settings, while also discussing inclusion concepts and optimization methods for faster linear responses and larger convergence regions. Finally, the theoretical content is summarized in the form of theorems and applied to test plants to validate the results, demonstrating the reduced conservatism of the proposed model compared to the standard quadratic Lyapunov approach and ensuring the proper inclusion of saturation. The conclusion synthesizes the main findings and highlights perspectives for future research and improvements.

1.1 Saturation

Physical systems are always subject to operational limitations. Among them, actuator saturation is a common case in which the actuator cannot exceed a certain level, whether in speed, power, angle, or any other physical quantity. When the control input exceeds this limit, the actuator simply delivers its maximum output, regardless of the actual command.

Because of that, saturation makes the system nonlinear, which limits the use of standard linear control techniques. Then, some possible strategies to handle saturation consist of:

I) Imposing the system to linearly evolve, which may reveal to be very conservative. It aims to keep the system operating within its linear region so that linear control techniques remain valid. Examples include oversizing the actuator or limiting the controller's performance. However, that usually increases energy and financial costs, but may reduce the performance of the closed loop.

II) Considering the possible saturation of the actuator and therefore the nonlinear behavior of the closed loop. In this report, we will follow this second direction, proposing methods to deal with the actuator saturation.

Another interesting way to handle the occurrence of input saturation lies in the design of additive loops as anti-windup compensator, only active when the saturation occurs. Thus, anti-windup emerges as a technique that modifies the control law to account for actuator limits ([2], [3]). It uses the control effort lost due to saturation, known as the dead-zone signal, as an additional input to the controller. As a result, when saturation occurs, a correction term is added to the control signal to compensate for the mismatch between the desired and actual inputs (see Fig. 2).

Despite all that, saturation is part of the reality we deal with in control systems. It affects how systems behave, how safe they are, and how far we can push their performance. That's why anti-windup techniques have gained so much recognition as a way to handle

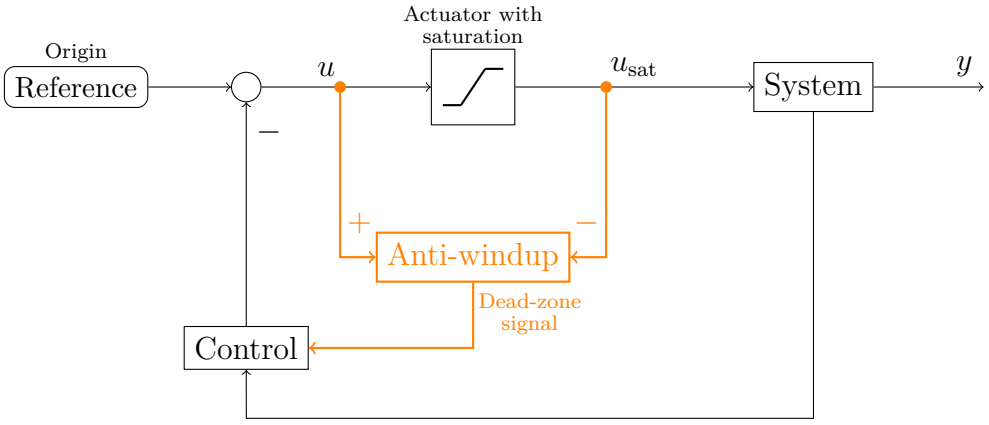

Figure 2: Anti-windup scheme with saturation compensation.

these limits. We see this in drones that stay under control even when actuators saturate [4], in marine robots that avoid overshoot [5], and in biomedical circuits that work safely [6]. That practical value is what motivates this work.

In the following of the report, we will present some techniques, based on recent advanced results for building Lyapunov functions [1], to handle linear plants subject to input saturation.

1.2 Stability

Stability refers to a system's ability to stay near or return to its equilibrium over time. If the system's states continuously approach the equilibrium point as time progresses, it is said to be asymptotically stable (See Chapter 4 [7]).

Several concepts are needed, as follows. The domain of attraction of the origin refers to the set of initial conditions from which the system is asymptotically stable at the origin. If this domain covers the entire state space, the system is considered globally asymptotically stable (GAS). When stability holds only in a restricted region, it is referred to as regionally (RAS) or locally (LAS) asymptotically stable. The exponential stablity can also be studied. In this case the basin of attraction of the origin is a subset of the state space.

In this context, the Lyapunov method is a key tool, as it allows stability analysis based on a function that captures the system's internal energy. Using this approach, one can derive mathematical conditions that ensure stability and provide an estimate of the basin of attraction. This formulation will be discussed in more detail in Section 3.1.

In many cases, these conditions lead to complex expressions that are difficult to handle directly. To address this, it is common to reformulate them as Linear Matrix Inequalities (LMIs), which make the problem more tractable through convex optimization techniques.

1.3 Systems under consideration

In this report we will study discrete-time systems described as follow:

$$\begin{cases} x((k+1)T_s) = Ax(kT_s) + Bu(kT_s), \\ y(kT_s) = Cx(kT_s) + Du(kT_s), \end{cases} \tag{1}$$

where $x(t)$, $u(t)$, and $y(t)$ denote the state, input, and output vectors at $t = kT_s$, with T_s representing the sampling period[1] and $k \in \mathbb{N}$ the discrete-time index. The matrices A, B, C, and D have compatible dimensions All further assumptions will be detailed in Section 2.1.

In the discrete-time case, stability is verified using the Schur–Cohn criterion, which requires all poles of the system to lie strictly inside the unit circle in the complex plane [8, Annexe C7.2]. This replaces the Hurwitz criterion used in continuous time, where stability is assessed by requiring all poles of the transfer function to lie in the open left half of the complex plane.

As will be discussed in Section 3.1, we assume that the closed-loop system without saturation, in its linear behavior, is stable before proposing the solution for the nonlinear case.

Notation

To simplify notation, the state at the next sampling instant $x((k+1)T_s)$ is written as $x[k+1]$ or simply x^+, and the state at the current instant $x(kT_s)$ as $x[k]$ or x. The control input $u(kT_s)$ is denoted by $u[k]$ or just u.

The dead-zone signal $\mathrm{dz}(u(x))$, which depends on the system state, is abbreviated to dz, and its value at the next instant $\mathrm{dz}(u(x^+))$ is written as dz^+.

In LMI expressions, the symbol $(\star)$ represents the symmetric term of a matrix, corresponding to the transposed block that completes the symmetric structure. The notation $\mathrm{He}(X)$ stands for the Hermitian part of a matrix: $\mathrm{He}(X) = X + X^\top$.

We use $\mathbb{R}^n$ for the n-dimensional real vector space, $\mathbb{R}^{n\times m}$ for real $n \times m$ matrices, S^n to denote the set of symmetric matrices of order n, and $\mathbb{D}^n$ for the set of diagonal matrices of order n. The identity matrix of size n is denoted by I_n.

For clarity, the symbols > 0 and < 0 refer to positive and negative scalar values, respectively, while $\succ 0$ and $\prec 0$ refer to positive and negative definite symmetric matrices, meaning that all their eigenvalues are strictly positive or negative.

2 Problem Formulation

2.1 System Description

A linear discrete-time system is described by:

$$x[k+1] = Ax[k] + Bu[k] \tag{2}$$

where $x[k] \in \mathbb{R}^n$ and $u[k] \in \mathbb{R}^m$ denote the system state and control input at the sampling instant kT_s, with $k \in \mathbb{N}$ and $T_s > 0$ representing the sampling period. The matrices A and B have appropriate dimensions and define the system dynamics, which are assumed to be stabilizable.

Considering that the control input u is subject to symmetric amplitude constraints, given by:

$$-1 \leq u \leq 1 \tag{3}$$

[1] See Appendix A.1.

Thus, it is possible to reformulate the system in order to explicitly account for input saturation as:

$$x[k+1] = Ax[k] + B\text{sat}(u[k]) \tag{4}$$

The function $\text{sat}(u[k])$, as represented in Fig. 3, denotes the symmetric saturation function applied to each component u_i of the control input, defined by:

$$\text{sat}_i(u) := \max\{-1, \min\{1, u_i\}\} \tag{5}$$

that is:

$$\text{sat}_i(u) = \begin{cases} 1, & \text{if } u_i \geq 1; \\ u_i, & \text{if } -1 \leq u_i \leq 1; \\ -1, & \text{if } u_i \leq -1. \end{cases} \tag{6}$$

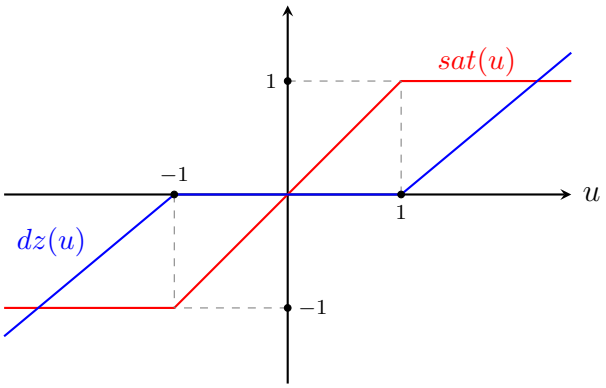

Figure 3: Saturation and dead-zone functions

Although the saturation bounds are initially assumed to be unitary for simplicity, the model in (4) can be generalized to account for arbitrary symmetric bounds by introducing a suitable gain factor into the matrix B[2].

The signal lost due to saturation is defined by the dead-zone function, as shown in Fig. 3, and expressed by:

$$\text{dz}(u[k]) = u[k] - \text{sat}(u[k]) \tag{7}$$

Thus,

$$dz_i(u) = \begin{cases} u_i - 1, & \text{if } u_i > 1; \\ 0, & \text{if } -1 \leq u_i \leq 1; \\ u_i + 1, & \text{if } u_i < -1. \end{cases} \tag{8}$$

To stabilize the system in the presence of input saturation, a nonlinear control law is introduced:

$$u[k] = K_1 x[k] + K_2 \text{dz}(u[k]) \tag{9}$$

where K_1 and K_2 are matrices of compatible dimensions. The presence of the K_2 term in the controller ensures the anti-windup behavior of the system, meaning that

[2]In industrial applications, actuator saturation limits are not always precisely known. In such cases, it is common to impose artificial conservative bounds to ensure that the true limits are fully contained.

the controller self-adjusts in the presence of saturation, preventing integrator windup or performance degradation due to the mismatch between desired and saturated control inputs.

The nonlinearity of the system arises from the nonlinear feedback loop induced by the control signal $u \mapsto \mathrm{dz}(u)$, which introduces the implicit dependence $x \mapsto u(x)$.

Thus, in the interval where the control signal is not saturated, i.e., $u_i \in [-1, 1]$, the system behaves linearly, since $\mathrm{dz}(u)$ is zero in this region. Similarly, by setting $K_2 = 0$, the system reduces to a classical linear analysis for any control signal.

The closed-loop system resulting from (4) and (9) reads:

$$x[k+1] = (A + BK_1)x[k] + B(K_2 - I_m)dz(u[k]) \tag{10}$$

The objective of this work is divided into two main problems:

1. Analysis: Given predefined matrices K_1 and K_2, assess the asymptotic stability of the closed-loop system (10).

2. Synthesis: Determine suitable matrices K_1 and K_2 ensuring the asymptotic stability of closed-loop system (10).

We will consider the two problems in the case of global and regional stability.

In this context, it is essential for the system to be well-posed in order to guarantee the existence of a unique solution to equation (9). Accordingly, all stability conditions proposed throughout this work are designed to satisfy the well-posedness requirements of the system (see Appendix A.2).

Additionally, a necessary condition for the stability of the saturated system is that the linear system without saturation is stable. This is ensured by requiring the matrix $A + BK_1$ to be Schur-Cohn, i.e., all its eigenvalues must lie strictly within the unit circle.

2.2 Closed-loop Dynamics

Based on the considerations above, the closed-loop system can be described by:

$$\begin{cases} x^+ = (A + BK_1)x + B(K_2 - I_m)\mathrm{dz}(u(x)) \\ u(x) = K_1 x + K_2 \mathrm{dz}(u(x)) \end{cases} \tag{11}$$

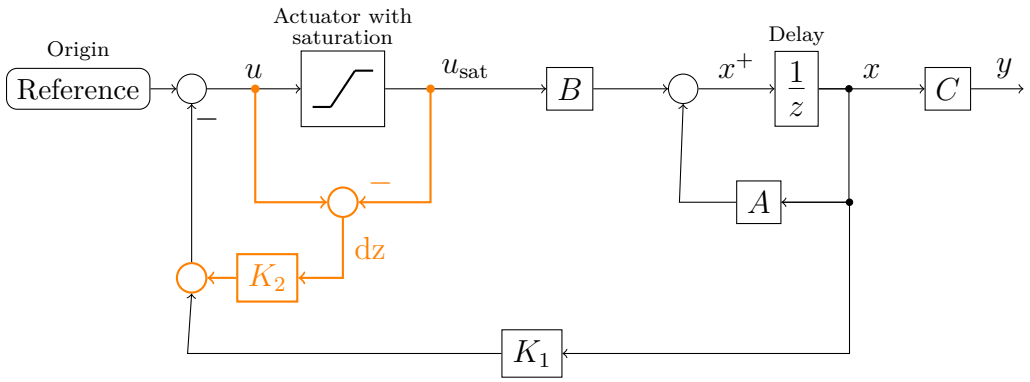

Figure 4: Proposed system diagram.

If asymptotic stability property holds for all initial states $x(0) \in \mathbb{R}^n$, the system is said to be globally asymptotically stable.

On the other hand, if the set of initial conditions ensuring stability is bounded, the problem also involves determining and enlarging the domain of attraction. In this case, the stability is referred to as regional asymptotic stability, which differs from local stability, where the attraction domain is assumed to be arbitrarily small.

The limitation on the domain of attraction arises from the presence of unstable eigenvalues in the open-loop system, that is, eigenvalues of matrix A located outside the unit circle [9].

Given that the domain of attraction is bounded, it is reasonable to restrict the analysis to this region. This approach provides greater flexibility, as it avoids imposing constraints beyond the system's intended operating range.

To reduce conservativeness, the analysis is restricted to a specific region of operation defined by (See [1]):

$$\mathcal{S}_h := \{x \in \mathbb{R}^n : |h(x)|_\infty \leq 1\} \tag{12}$$

The boundaries of this set are not necessarily linear. The function $h(x)$ defines the shape of the boundary as:

$$h(x) = H_1 x + H_2 \mathrm{dz}(u(x)) \tag{13}$$

where the matrices H_1 and H_2 have compatible dimensions. In the particular case where $H_1 = 0$ and $H_2 = 0$, the function $h(x)$ vanishes for all x, and the analysis reduces to the global case.

3 Sign-Indefinite Lyapunov Function

3.1 Proposed Structure

In the classical Lyapunov approach, the stability of a nonlinear system is studied through an energy-like function $V(x)$. According to Lyapunov's theorem, if this function is always positive and decreases along the system trajectories, then the system tends to move toward its equilibrium point.

In discrete time, these conditions are expressed as follows [3] [4]:

$$\begin{cases} (1) \quad V(x) > 0, \quad \forall x \neq 0; \\ (2) \quad \Delta V(x) < 0, \quad \forall x \neq 0; \\ (3) \quad V(0) = 0. \end{cases} \tag{14}$$

A common choice for the Lyapunov function is the quadratic form $V_L(x) = x^\top P_L x$, where P_L is known as the Lyapunov matrix. A direct way to certify the stability of the closed loop (11) is to find a matrix P_L that is symmetric and positive definite, satisfying some matrix inequlity conditions (see, for example [8]).

[3] If the equilibrium point is not at the origin, a standard approach is to shift the system's coordinates accordingly [10].

[4] If the equilibrium point varies over time, the system can be rewritten relative to a reference trajectory. This modeling approach is useful, for instance, when designing controllers for trajectory segments (See [11]).

The main contribution of this work is to extend the already powerful standard Lyapunov approach by allowing the associated matrix to be sign-indefinite, thus extending the results obtained in [1] for saturated continuous-time systems. This added flexibility enables less conservative stability conditions while still ensuring asymptotic stability, potentially leading to more efficient results.

In this context, the chosen structure of the Lyapunov function is defined as[5]:

$$V(x) = \begin{bmatrix} x \\ dz(u(x)) \end{bmatrix}^\top \begin{bmatrix} P_0 & P_1 \\ P_1^\top & P_2 \end{bmatrix} \begin{bmatrix} x \\ dz(u(x)) \end{bmatrix} = \begin{bmatrix} x \\ dz \end{bmatrix}^\top P \begin{bmatrix} x \\ dz \end{bmatrix} \tag{15}$$

Here, P_0 reflects the stability of the closed-loop system without saturation. Since it is natural to require the unsaturated system to be stable, P_0 is chosen to be symmetric and positive definite. This is equivalent to assuming that $(A + BK_1)$ is a Schur-Cohn matrix, meaning all its eigenvalues lie strictly inside the unit circle.

The full matrix P, however, is not required to be positive definite. It will be shown that $V(x)$ is required to be positive only in a certain region of the state space.

Due to limitations of the system itself, there are cases where the controller cannot guarantee asymptotic stability from all initial conditions. In such cases, the goal is to find the largest set of initial conditions that still ensures convergence. These situations are referred to as regional cases, as discussed in Section 2.2.

In the regional case, since the domain is limited, stability properties are established only within the operating region. This leads to a less conservative approach, as the analysis does not require conditions to hold globally. Therefore, the domain of asymptotic stability is defined entirely within the set given by equation (13), and the focus is on ensuring that the desired properties hold within this region. Compared to the global case, it is also necessary to define the matrices H_1 and H_2.

Using the S-procedure, the basic Lyapunov inequalities can be reformulated in an extended form that incorporates both the system dynamics and sector conditions (see Section 2.6.3 in [12]). As will be detailed in Section 3.2, this approach introduces additional degrees of freedom.

As a result, it becomes possible to obtain LMIs that guarantee asymptotic stability, even when the associated Lyapunov matrix is not positive definite.

3.2 System Properties

In the global setting, it can be observed that the dead-zone function $dz(u)$ and the saturation function $\text{sat}(u)$ have the same sign, componentwise. This property, illustrated in Fig. 3 and derived from equations (6) and (8), leads to the classical sector condition used in many LMI-based stability formulations (see [9], [1]):

$$dz^\top T_1 \,\text{sat}(u) \geq 0, \tag{16}$$

where $T_1 \in \mathbb{D}^m_{\geq 0}$ is a symmetric positive semidefinite diagonal matrix.

To extend the global sector condition to a regional context, we consider the operating region defined by the set $\mathcal{S}_h$. Within this region, a generalized sector condition can be formulated as [1], [8]:

$$dz^\top T_1 \left(\text{sat}(u) - h(x)\right) \geq 0, \tag{17}$$

[5]Note that dz stands for $dz(u(x))$, which is implicitly state-dependent.

for all $x \in \mathcal{S}_h$, where $T_1 \in \mathbb{D}^m_{\succeq 0}$ is a diagonal positive-definite matrix. This regional condition is illustrated in Fig. 21, see also Appendix A.3 for a more detailed explanation.

This regional sector condition generalizes the global case. In particular, setting $H_1 = 0$ and $H_2 = 0$ in (13) recovers the global condition (16).

By restricting the sector condition to the region $\mathcal{S}_h$, the Lyapunov function $V(x)$ only needs to be positive definite within this set. Outside of it, $V(x)$ is allowed to be indefinite or even negative. This added flexibility in the definition of V increases the freedom to choose the matrix P, which often leads to less conservative results and broader estimates of the region of attraction.

Additionally, by analyzing the variation of the saturation signal, the following property can be established (see Appendix A.4 for a detailed analysis):

$$(\Delta dz)^\top T\, \Delta\mathrm{sat}(u) \;\geq\; 0, \tag{18}$$

where

$$\Delta dz = dz(u^+) - dz(u), \qquad \Delta\mathrm{sat}(u) = \mathrm{sat}(u^+) - \mathrm{sat}(u).$$

As shown in Appendix A.4, this property can be decoupled into two separate inequalities, each associated with a distinct matrix, T_2 and $T_3 \in \mathbb{S}^m_{\succ 0}$, thus increasing the degrees of freedom in the formulation.

The inequalities (17) and (18) can be equivalently expressed as the following LMIs, respectively:

$$\begin{bmatrix} x \\ dz \end{bmatrix}^\top \begin{bmatrix} 0 & 0 \\ T_1(K_1 - H_1) & T_1(K_2 - I_m - H_2) \end{bmatrix} \begin{bmatrix} x \\ dz \end{bmatrix} \geq 0 \tag{19}$$

$$\begin{bmatrix} x \\ dz \\ dz^+ \end{bmatrix}^\top \begin{bmatrix} 0 & 0 & 0 \\ -T_3K_1(A + BK_1 - I_n) & -T_3(K_1B - I_m)(K_2 - I_m) & -T_3(K_2 - I_m) \\ T_2K_1(A + BK_1 - I_n) & T_2(K_1B - I_m)(K_2 - I_m) & T_2(K_2 - I_m) \end{bmatrix} \begin{bmatrix} x \\ dz \\ dz^+ \end{bmatrix} \geq 0 \tag{20}$$

3.3 Stability Conditions

3.3.1 Unsaturated system

The system described in (11) can be interpreted as a combination of the linear behavior without saturation, given by $(A+BK_1)x$, and the nonlinear effect of saturation, captured by the term $B(K_2 - I_m)dz(u(x))$ (See Fig. 5).

We assume that the unsaturated system is stabilizable by state feedback. That is, the matrix $A + BK_1$ is Schur-Cohn, meaning all its eigenvalues lie strictly inside the unit circle. Under this assumption, the discrete-time closed-loop system without saturation is asymptotically stable.

This stability implies the existence of a quadratic Lyapunov function of the form:

$$V_0(x) = x^\top P_0 x, \qquad P_0 \succ 0, \tag{21}$$

such that its variation along trajectories satisfies:

$$\Delta V_0 = x^{+\top} P_0 x^+ - x^\top P_0 x < 0, \tag{22}$$

where $x^+ = (A + BK_1)x$ denotes the next state. This represents the behavior of the system in the absence of saturation, meaning that the control input is fully applied and the dead-zone component satisfies $dz(u) = 0$.

This leads to the discrete-time Lyapunov inequality:

$$(A + BK_1)^\top P_0 (A + BK_1) - P_0 \prec 0. \tag{23}$$

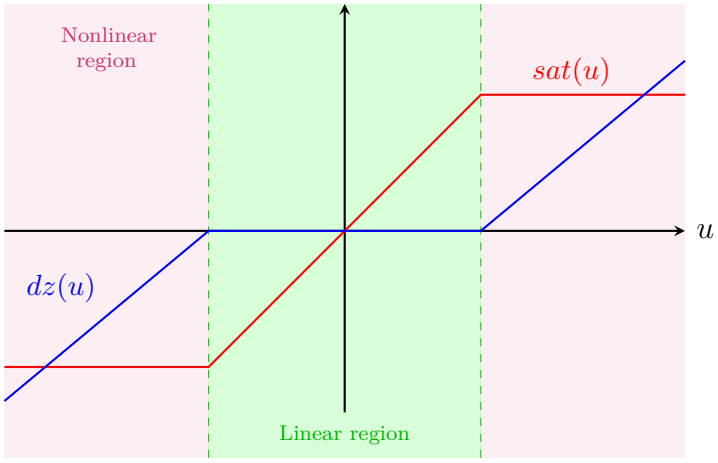

Figure 5: Linear and nonlinear regions of the control signal.

However, the condition that $A + BK_1$ is Schur-Cohn only ensures local asymptotic stability of the origin. This means that the system is guaranteed to converge to the origin only for initial conditions sufficiently close to it.

To enlarge the region of attraction and address the nonlinear effects of input saturation, it is beneficial to formulate more refined conditions that ensure regional or even global stability. This motivates the developments presented in the next sections.

3.3.2 Extended Lyapunov Function

One way to incorporate the nonlinear effects into the energy-based analysis is by using the extended quadratic form (15). However, as one of the main goals of this work is to allow the matrix P_2 to be sign-indefinite, the function $V(x)$ alone does not guarantee positivity.

However, by applying the S-procedure and the sector condition introduced in Section 3.2, it is possible to establish a sufficient condition that ensures the positivity of $V(x)$.

In particular, if the following inequality holds:

$$V(x) > V(x) - \mathrm{He}\left(dz^\top T_1(\mathrm{sat}(u) - h(x))\right) > 0, \tag{24}$$

then $V(x)$ is positive definite within the region $\mathcal{S}_h$.

By rewriting this condition in matrix form, we obtain the first condition, which consists in a positivity condition for the function V:

$$\begin{bmatrix} P_0 & * \\ P_1^\top - T_1(K_1 - H_1) & P_2 - He(T_1(K_2 - I_m - H_2)) \end{bmatrix} \succ 0 \tag{25}$$

with $T_1 \in \mathbb{S}^m_{\succ 0}$. As previously discussed, setting $H_1 = 0$ and $H_2 = 0$ extends this condition to the global case.

This first condition serves as the foundation for all cases studied in this work. Modifications such as introducing auxiliary variables are applied to preserve convexity, but the core structure remains unchanged.

3.3.3 Inclusion Condition

In the context of regional solutions, it is essential to ensure that the asymptotic stability region lies entirely within the domain $\mathcal{S}_h$, since the sector conditions (17) are only guaranteed to hold inside this region.

This requirement reflects the nature of the controller's operating region, which imposes two types of constraints: an energy bound on the system states and a saturation limit on the control input.

The energy constraint is expressed by the set:

$$S(V, r^{-1}) = \left\{ x \in \mathbb{R}^n \,;\, \begin{bmatrix} x \\ dz(x) \end{bmatrix}^\top P \begin{bmatrix} x \\ dz(x) \end{bmatrix} \leq r^{-1} \right\} \tag{26}$$

where we assume $r^{-1} > 0$ represents the maximum admissible energy in the system.

The control input constraint, on the other hand, is described by:

$$S(H, u_0) = \{x_i \,;\, |h(x_i)| \leq u_{0i},\ \forall i \in \mathbb{N}\} \tag{27}$$

where u_0 denotes the componentwise saturation limits of the control input.

To ensure that the Lyapunov-based analysis is valid throughout the entire region of operation, we seek to verify the inclusion:

$$S(V, r^{-1}) \subseteq S(H, u_0)$$

The region inside $\mathcal{S}_h$ that ensures convergence will be denoted by $W(x)$:

$$W(x) = \begin{cases} min\{V(x), 1\}, & \text{for } x \text{ in } \mathcal{S}_h \\ 1, & \text{otherwise.} \end{cases}$$

To translate this inclusion into an LMI formulation, we begin by expressing the saturation bounds componentwise. For each control input, we introduce a generic limit $u_{0i} > 0$, which will later be assumed equal to one without loss of generality, as discussed in Section 2.1.

Based on the expression for $h(x)$ in (13), the condition (27) can be expanded as:

$$|h(x_i)|^2 = (H_{1i}x + H_{2i}dz)^\top (H_{1i}x + H_{2i}dz) \leq u_{0i}^2$$

where, H_{1i} and H_{2i} denote the i-th row of the matrices H_1 and H_2, respectively. Analyzing the condition row by row, rather than treating the entire matrix expression as a whole, provides greater flexibility in the design.

As a result, the condition can be written as the following quadratic inequality:

$$\begin{bmatrix} x \\ dz(x) \end{bmatrix}^\top \left(\frac{1}{u_{0_i}^2} \begin{bmatrix} H_{1_i}^\top \\ H_{2_i}^\top \end{bmatrix} \begin{bmatrix} H_{1i} & H_{2i} \end{bmatrix} \right) \begin{bmatrix} x \\ dz(x) \end{bmatrix} < 1$$

To ensure that $S(V, r^{-1}) \subseteq S(H, u_0)$, we establish the following inequality,

$$\begin{bmatrix} x \\ dz(x) \end{bmatrix}^\top \left(\frac{1}{u_{0_i}^2} \begin{bmatrix} H_1^\top \\ H_2^\top \end{bmatrix} \begin{bmatrix} H_1 & H_2 \end{bmatrix} \right) \begin{bmatrix} x \\ dz(x) \end{bmatrix} \leq \begin{bmatrix} x \\ dz(x) \end{bmatrix}^\top rP \begin{bmatrix} x \\ dz(x) \end{bmatrix}$$

This condition is both valid and sufficient, since it implies that whenever the second inequality in the previous expression holds, the first one does as well. As a result, we obtain:

$$0 \leq \begin{bmatrix} x \\ dz(x) \end{bmatrix}^\top \left(P - \begin{bmatrix} H_{1_i}^\top \\ H_{2_i}^\top \end{bmatrix} \frac{1}{ru_{0_i}^2} \begin{bmatrix} H_{1i} H_{2i} \end{bmatrix} \right) \begin{bmatrix} x \\ dz(x) \end{bmatrix}$$

Based on Schur complement (see Note 1), and assuming that $r, u_{0_i} > 0$ are fixed, we can derive the following matrix inequality that guarantees inclusion within the operating region.

$$\left[\begin{array}{cc:c} P_0 & P_1 & H_{1i}^\top \\ P_1^\top & P_2 & H_{2i}^\top \\ \hdashline H_{1i} & H_{2i} & ru_{0_i}^2 \end{array}\right] \succeq 0$$

This condition ensures that $V(x)$ is positive within the region where the sector condition is valid. Outside this region, positivity is not required, which introduces additional degrees of freedom and can result in less conservative, more effective designs. Based on this idea, we update condition (25), initially defined to guarantee positivity, so that it also accounts for the inclusion constraint. This leads to the following **inclusion condition**:

$$\left[\begin{array}{cc:c} P_0 & P_1 - (K_1 - H_1)^\top T_1 & H_{1i}^\top \\ P_1^\top - T_1(K_1 - H_1) & P_2 - He(T_1(K_2 - I_m - H_2)) & H_{2i}^\top \\ \hdashline H_{1i} & H_{2i} & ru_{0_i}^2 \end{array}\right] \succeq 0 \tag{28}$$

By setting $ru_{0_i}^2 = 1, \forall i \in \{1, \ldots, m\}$ and $H_1, H_2 = 0$, we recover the original condition (25), showing that (28) extends the classical formulation by explicitly including the regional constraint.

For simplicity, and without loss of generality, we assume $ru_0^2 = 1$ in the synthesis case.

Note 1 – Schur Complement

The Schur complement is a fundamental tool in matrix analysis that allows block matrix inequalities to be simplified. Given a symmetric block matrix:

$$M = \begin{bmatrix} A & B \\ B^\top & C \end{bmatrix},$$

the condition $M \succ 0$ is equivalent to:

- $C \succ 0$ and
- $A - BC^{-1}B^\top \succ 0$.

This transformation helps express matrix inequalities as LMIs. See Chapter 2 of [12] for more detailed information.

3.3.4 Extended Lyapunov Variation

In order to ensure stability, it is necessary that the variation of the Lyapunov function satisfies:

$$\triangle V(x) < 0$$

By expanding the variation of the extended Lyapunov function in matrix form, we obtain:

$$\triangle V(x) = \begin{bmatrix} x^+ \\ dz^+(x) \end{bmatrix}^\top \begin{bmatrix} P_0 & P_1 \\ P_1^\top & P_2 \end{bmatrix} \begin{bmatrix} x^+ \\ dz^+(x) \end{bmatrix} - \begin{bmatrix} x \\ dz(x) \end{bmatrix}^\top \begin{bmatrix} P_0 & P_1 \\ P_1^\top & P_2 \end{bmatrix} \begin{bmatrix} x \\ dz(x) \end{bmatrix}$$

Rewriting this expression leads to a quadratic form in the extended state vector:

$$\triangle V(x) = \begin{bmatrix} x \\ dz(x) \\ dz^+(x) \end{bmatrix}^\top \begin{bmatrix} M_{11} & * & * \\ M_{21} & M_{22} & * \\ P_1^\top(A + BK_1) & P_1^\top B(K_2 - I_m) & P_2 \end{bmatrix} \begin{bmatrix} x \\ dz(x) \\ dz^+(x) \end{bmatrix} \tag{29}$$

where

- $M_{11} = (A + BK_1)^\top P_0 (A + BK_1) - P_0$
- $M_{21} = (K_2 - I_m)^\top B^\top P_0 (A + BK_1) - P_1^\top$
- $M_{22} = (K_2 - I_m)^\top B^\top P_0 B (K_2 - I_m) - P_2$

where $P_0 \in \mathbb{S}^n_{\succ 0}$, $P_1 \in \mathbb{R}^{n \times m}$ and $P_2 \in \mathbb{S}^m$. However, since the matrix P_2 is not constrained to be positive definite, this expression alone does not guarantee negativity of $\Delta V(x)$. To overcome this, we once again apply the S-procedure using the sector conditions introduced in Section 3.2.

Specifically, we consider the following relaxed condition:

$$\triangle V < \triangle V + \mathrm{He}[dz^\top T_1(\mathrm{sat}(u) - h(x)) + (dz^+)^\top T_2\,\Delta\mathrm{sat}(u) - dz^\top T_3\,\Delta\mathrm{sat}(u)] < 0$$

which introduces additional degrees of freedom through the diagonal matrices T_1, T_2, and $T_3 \in \mathbb{S}^m_{\succ 0}$.

Expanding this inequality leads to the **second stability condition** of the system:

$$\begin{bmatrix} M_{11} & * & * \\ M_{21} & M_{22} & * \\ P_1^\top(A+BK_1) & P_1^\top B(K_2 - I_m) & P_2 \end{bmatrix} + \mathrm{He}\left(\begin{bmatrix} 0 \\ T_1 \\ 0 \end{bmatrix} \begin{bmatrix} K_1 - H_1 & M_3 - H_2 & 0 \end{bmatrix} + \begin{bmatrix} 0 \\ 0 \\ T_2 \end{bmatrix} \begin{bmatrix} M_1 & M_2 & M_3 \end{bmatrix} - \begin{bmatrix} 0 \\ T_3 \\ 0 \end{bmatrix} \begin{bmatrix} M_1 & M_2 & M_3 \end{bmatrix} \right) \prec 0 \tag{30}$$

where

- $M_1 = K_1(A + BK_1 - I_n)$
- $M_2 = (K_1B - I_m)(K_2 - I_m)$
- $M_3 = (K_2 - I_m)$

As with the first condition, equation (30) provides the foundation for the next steps in both the analysis and synthesis settings, as it characterizes the negative variation of the Lyapunov function. As such, it will be reformulated with appropriate variable substitutions to maintain convexity in the optimization process.

3.4 Convex Reformulation

Convexity is a key property in optimization problems, as it ensures that all solutions lie within a single convex set. This eliminates the presence of multiple local minima or maxima, avoiding peaks, valleys, or discontinuities in the solution space.

To preserve this property, it is crucial to avoid products between decision variables. Consequently, certain nonlinear terms involving controller gains and sector condition matrices must be reformulated using auxiliary variables.

In the analysis case, the following substitutions are introduced:

$$\begin{cases} Z_1 = T_1 H_1 \\ Z_2 = T_1 H_2 \end{cases} \tag{31}$$

In the synthesis cases, to reduce the number of such variables, all sector condition matrices T_1, T_2, T_3, and $\hat{T}$, that will be introduced in (39), are identical. Since all matrices T are diagonal and positive, they are invertible, so we can define $S = T^{-1}$, which also remains positive definite.

The following auxiliary variables are then introduced:

$$\begin{cases} Z_1 = H_1 M \\ Z_2 = H_2 S \\ Y_1 = K_1 M \\ Y_2 = K_2 S \end{cases} \tag{32}$$

where $M \in \mathbb{R}^{m \times m}$ is a non-singular auxiliary matrix. Moreover, introducing M and S implies a change of variables in the Lyapunov function matrix (15):

$$\begin{cases} Q_0 = M^\top P_0 M \\ Q_1 = M^\top P_1 M \\ Q_2 = S^\top P_2 S \end{cases} \tag{33}$$

These substitutions enable a fully linear formulation of the LMIs, ensuring that all constraints remain convex and efficiently solvable.

Reformulation for Synthesis

To further simplify the formulation, the second stability condition (29) in the synthesis case is expressed in terms of the extended state vector $\eta = \begin{bmatrix} x; & dz; & x^+; & dz^+ \end{bmatrix}$, allowing for a reduced number of auxiliary variables while preserving convexity.

Based on the reformulations introduced earlier, the stability conditions (28) and (30) can be post- and pre-multiplied by $\mathrm{diag}(M, S)$ and its transpose, respectively, and then rearranged. This leads to the following expressions:

$$\begin{bmatrix} Q_0 & Q_1 & 0 \\ Q_1^\top & Q_2 & 0 \\ 0 & 0 & 1 \end{bmatrix} + \mathrm{He}\left(\begin{bmatrix} 0 & Z_1^\top - Y_1^\top & Z_{1i}^\top \\ 0 & Z_2 - Y_2 + S & Z_{2i}^\top \\ 0 & 0 & 0 \end{bmatrix} \right) \succ 0 \tag{34}$$

$$\begin{bmatrix} -Q_0 & -Q_1 & 0 & 0 \\ -Q_1^\top & -Q_2 & 0 & 0 \\ 0 & 0 & Q_0 & Q_1 \\ 0 & 0 & Q_1^\top & Q_2 \end{bmatrix} + \begin{bmatrix} 0 & * & * & * \\ 2Y_1 - Z_1 & \mathrm{He}(2Y_2 - Z_2) - 4S & * & * \\ AM + BY_1 & -Y_1^\top + B(Y_2 - S) & \mathrm{He}(M) & * \\ -Y_1 & -\mathrm{He}(Y_2) + 2S & Y_1 & \mathrm{He}(Y_2) - 2S \end{bmatrix} \prec 0 \tag{35}$$

Here, Z_{1i} denotes the i-th row of matrix Z_1, and similarly for Z_2. For clarity, the complete derivation of (35) is provided in Appendix A.5.

Recall that the global synthesis case is a particular instance of the regional formulation, where H_1 and H_2 are set to zero (see Appendix A.3). In this case, conditions (34) and (35) reduce to the global form with $Z_1 = 0$ and $Z_2 = 0$.

3.5 Optimization

3.5.1 Decay rate

Pole placement is a well-established and effective strategy for shaping the dynamic response of linear systems.

In the absence of saturation, it allows us to guarantee a minimum convergence rate by placing all eigenvalues of the closed-loop matrix $A+BK_1$ (See (11)) inside a disk of radius $r < 1$ in the complex plane. The smaller the value of r, the faster the system converges to the origin, as shown in Fig. 17.

This approach will therefore be used to optimize the controller design in both the global and regional synthesis cases.

According to Theorem 2.2 in [13], if the spectral radius of a matrix M, defined as the largest magnitude among its eigenvalues, is less than a given scalar $r > 0$, then there exists a symmetric positive definite matrix R such that:

$$\left(\tfrac{M}{r}\right)^\top R \left(\tfrac{M}{r}\right) - R < -I < 0.$$

In our application, the matrix M corresponds to the unsaturated system ($dz = 0$), and is given by $A + BK_1$. Therefore, the condition becomes:

$$(A + BK_1)^\top R(A + BK_1) < r^2 R.$$

This inequality guarantees an energy decay rate of r^2, which implies that all eigenvalues of $A + BK_1$ lie strictly inside the disk of radius r in the complex plane.

Using the Schur complement and assuming that R is positive definite (and thus invertible), the condition above is equivalent to the following LMI:

$$\begin{bmatrix} r^2 R & (A + BK_1)^\top \\ A + BK_1 & R^{-1} \end{bmatrix} \succ 0$$

By introducing the change of variable $R^{-1} = \bar{R}$ and post- and pre-multiplying the inequality by $\mathrm{diag}(M^\top, I)$ and $\mathrm{diag}(M, I)$, we obtain:

$$\begin{bmatrix} r^2 M^\top R M & M^\top (A + BK_1)^\top \\ (A + BK_1)M & R^{-1} \end{bmatrix} \succ 0$$

Using inequality Note 2,we ensure that the following LMI guarantees all eigenvalues of the closed-loop system lie within the disk of radius r:

$$\begin{bmatrix} r^2(M + M^\top - \bar{R}) & M^\top (A + BK_1)^\top \\ (A + BK_1)M & \bar{R} \end{bmatrix} \succ 0 \tag{36}$$

Therefore, we include condition (36) as an additional constraint in our LMI formulation to ensure a minimum convergence rate for the unsaturated system.

Note 2

For $R \succ 0$, the inequality

$$(R^{-1} - M)^\top R(R^{-1} - M) \succeq 0$$

is always satisfied, since it corresponds to a positive quadratic form. Expanding and rearranging yields the relaxed condition:

$$M^\top R M \succeq M + M^\top - R^{-1}. \tag{37}$$

3.5.2 Regional Domain Maximization

In the regional case, the goal is to ensure that the domain of attraction is as large as possible while still guaranteeing convergence to the equilibrium point, since a larger region means more initial states are guaranteed to converge.

An auxiliary quadratic function $\hat{V}(x)$ is introduced as a Lyapunov candidate to describe the system's behavior in the unsaturated regime:

$$\hat{V}(x) = x^\top \hat{P} x \tag{38}$$

The objective is to inscribe the ellipsoid $\varepsilon(\hat{P}, 1)$ within the region of convergence and to maximize its volume [8]. This can be accomplished by minimizing the matrix $\hat{P} \in \mathbb{S}^n$, which determines the ellipsoid's shape and size:

$$\varepsilon(\hat{P}, 1) := \{x \in \mathbb{R}^n : x^\top \hat{P} x < 1\} \subset S(V, 1)$$

To ensure that the ellipsoid is entirely contained within the region $\mathcal{S}_h$, we impose the inequality

$$V(x) < x^\top \hat{P} x\,, \quad \forall x \in \mathcal{S}_h$$

where $V(x)$ is defined in (15). By incorporating the regional sector condition (48), this inequality can be rewritten as:

$$0 < x^\top \hat{P} x - V(x) - \mathrm{He}\left(dz^\top \hat{T}(sat(u) - h(x))\right)$$

By expanding this inequality, we obtain the following matrix condition:

$$\begin{bmatrix} \hat{P} - P_0 & * \\ -(P_1^\top + (K_1 - H_1)\hat{T}) & -(P_2 + \mathrm{He}(\,\hat{T}(K_2 - I_m - H_2)\,)) \end{bmatrix} \succeq 0 \tag{39}$$

By minimizing $\hat{P}$, we obtain a larger ellipsoid and, consequently, a broader estimate of the domain of attraction within $\mathcal{S}_h$. Therefore, the trace of $\hat{P}$ is included as the objective function to be minimized, subject to the previously defined stability conditions.

As detailed in section 3.4, this condition can be further expanded for the synthesis case, leading to the following LMI:

$$\begin{bmatrix} \mathrm{He}(M) - Q_0 & * & * \\ I_n & \hat{P} & * \\ -Q_1^\top - Y_1 + Z_1 & 0 & -Q_2 - \mathrm{He}(Y_2 - Z_2) + 2S \end{bmatrix} \succeq 0 \tag{40}$$

The full derivation of this condition is provided in Appendix A.5.

4 Results

The codes developed during this internship, available in the repository [14], are organized into modular functions, which makes them easier to adapt and reuse.

The theoretical results introduced earlier are now presented in theorem form to provide a clearer view of the proposed framework and how it is applied.

As mentioned before, some optimization procedures can be included. These are optional, but they are highly recommended because they often lead to more accurate and reliable results.

After completing the synthesis process, an analysis will always be carried out based on the obtained controller. This is because, in the synthesis, the inclusion of matrix S makes the result more conservative and, therefore, performing the analysis allows for more optimized results.

In the implementation, due to numerical issues inherent to the use of LMI solvers, a safety factor will be applied so that, instead of checking whether the condition is positive, it must be greater than a positive constant. The same applies to the analysis of the negativity of a condition. The proposed approach is that the value of this constant is chosen solely to avoid scaling problems between the terms, therefore it is selected to be sufficiently small so as not to affect the obtained result.

4.1 Global Results

4.1.1 Global Analysis

Theorem 1: Global Analysis

Given control gains K_1 and K_2, if there exist matrices $P_0 \in \mathbb{S}^n_{\succ 0}$, $P_1 \in \mathbb{R}^{n\times m}$, $P_2 \in \mathbb{S}^m$, $T_1, T_3 \in \mathbb{D}^n_{\succeq 0}$, and $T_2 \in \mathbb{D}^n_{\succ 0}$ satisfying conditions (25) and (30), under the assumption that H_1 and H_2 are null, then the origin of system (11) is GAS.

Example 1) This example is based on the work presented in [15], which investigates the control of the angular speed of a permanent magnet direct current motor. The goal is to regulate the shaft rotation by applying a suitable armature voltage, allowing the motor to follow a given speed reference with accuracy, and Fig. 6 presents the electrical diagram of the motor, emphasizing the main physical quantities that define the model.

The system modeling starts from the continuous-time formulation and is represented by the matrices given in (41), which are associated with the state-space system described in (45) in Appendix A.1. The numerical parameters used in the simulation are listed in Table 1.

$$A_c = \begin{bmatrix} -b_m/J & K_m/J \\ K_b/L_a & -R_a/L_a \end{bmatrix}; \quad B_c = \begin{bmatrix} 0 \\ 1/L_a \end{bmatrix}; \quad T_s = 0.8s; \tag{41}$$

$$K_1 = \begin{bmatrix} -0.0009 & -0.2294 \end{bmatrix}; \qquad K_2 = -0.2246;$$

The sampling time was chosen according to the procedure described in Section 1.3, ensuring that the discretization remains faithful to the continuous model. The gains K_1 and K_2 were determined through the global synthesis process.

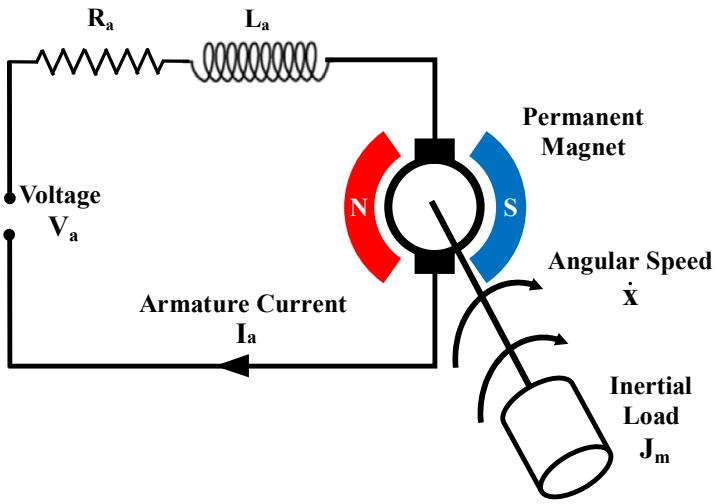

Figure 6: Electrical diagram of Example 1. Adapted from [16].

Parameter	**Value**
Resistance of armature, R_a	1 Ω
Inductance of armature, L_a	0.5 H
Inertia of Rotor, J	0.01 kg m^2
Coefficient of Viscous friction, b_m	0.1 N m s/rad
Torque constant, K_m	0.01 N m/A
Counter emf constant, K_b	0.01 s/rad

Table 1: Motor parameters

Through the analysis process, it was possible to obtain a Lyapunov matrix that is not positive definite (as intended in this work) while still ensuring the stability of the system. Following the structure of Equation (15), it can be seen that the submatrix P_0 is positive definite, whereas P_2 is negative definite.

$$P = \begin{bmatrix} 11.1918 & -0.0004 & -0.2710 \\ -0.0004 & 11.2944 & 0.3265 \\ -0.2710 & 0.3265 & -7.6409 \end{bmatrix}$$

Allowing the Lyapunov matrix to be non-positive definite provides greater degrees of freedom in the design, representing a significant step toward the development of future control methods.

The open-loop pole allocation analysis shows that both poles lie inside the unit circle, satisfying the Schur–Cohn criterion and indicating that the system is globally stable. Even in this condition, it is possible to design a controller to increase the speed of the system's linear response, as illustrated in Fig. 7a.

This global stability is further evidenced by the phase portrait in Fig. 7b, where the state trajectories, starting from different initial conditions, converge toward the origin.

The consistent convergence across the state space reinforces the global nature of the stability.

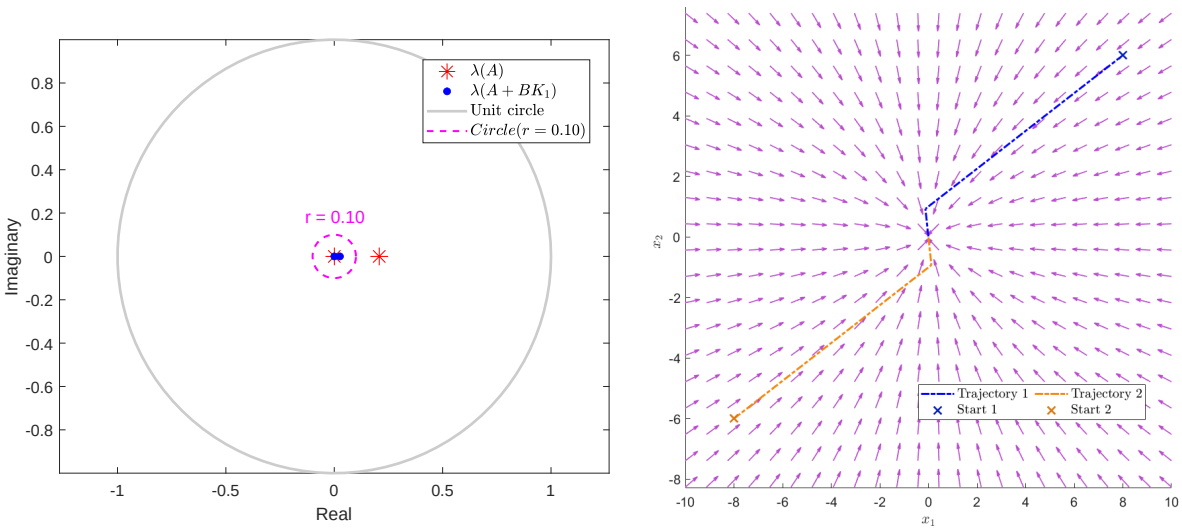

(a) Pole placement. (b) State convergence.

Figure 7: Closed-loop behavior of the DC motor system.

Finally, this property is also reflected in the Lyapunov function, which remains positive throughout the entire domain, as shown in Fig. 8. Together, these results confirm the global character of the system and the validity of the stability analysis.

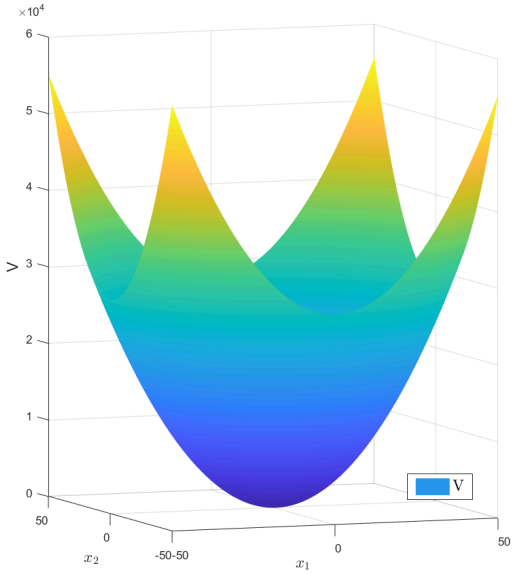

Figure 8: Positive Lyapunov function for Example 42.

4.1.2 Global Synthesis

Theorem 2: Global Synthesis

If there exist matrices $Q_0 \in \mathbb{S}^n_{\succ 0}$, $Q_1 \in \mathbb{R}^{n\times m}$, $Q_2 \in \mathbb{S}^m$, $S \in \mathbb{D}^n_{\succ 0}$, $M \in \mathbb{R}^{n\times n}$, $Y_1 \in \mathbb{R}^{m\times n}$, and $Y_2 \in \mathbb{R}^{m\times m}$ satisfying conditions (34) and (35), with Y_1, Y_2, $Z_1 = 0$, $Z_2 = 0$ and Q_0, Q_1 and Q_2 defined as in (33), then the origin of system (11) is GAS with the gains $K_1 = Y_1 M^{-1}$ and $K_2 = Y_2 S^{-1}$.

Optimization

To increase the **decay rate** of the system in the absence of saturation, one may include the additional condition (36), assuming $r \in [0, 1]$ and $R \in \mathbb{S}^n_{\succ 0}$.

Example 2) Consider the example corresponding to the continuous-time system (45, Appendix A.1) with the matrices:

$$A_c = \begin{bmatrix} -2 & -0.02 \\ 1 & -0.1 \end{bmatrix}; \quad B_c = \begin{bmatrix} 2 \\ 0 \end{bmatrix}; \quad T_s = 0.8s; \tag{42}$$

Through the synthesis procedure, the following controller gains were obtained:

$$K_1 = \begin{bmatrix} -0.5143 & -1.0217 \end{bmatrix}; \qquad K_2 = -1.1844;$$

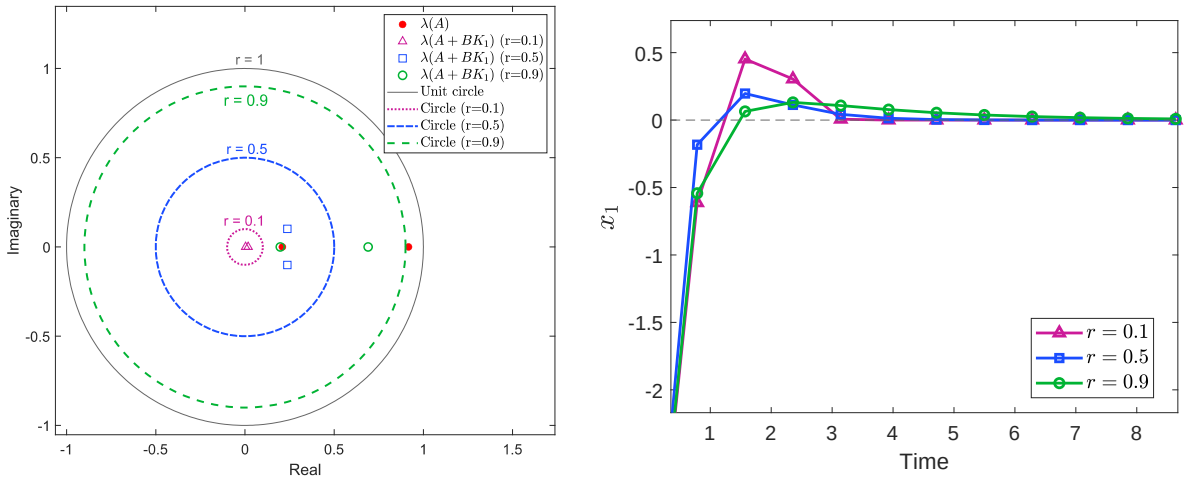

(a) Pole placement.

(b) State convergence.

Figure 9: Results for different decay rates r.

In addition, the optimization process can be used to place the closed-loop poles in order to achieve a faster response in the linear operating region, as shown in Fig. 9.

However, it is important to note that increasing the response speed may also intensify the windup effect, as illustrated in Fig. 9b.

The saturation effect can be observed in the control signal in Fig. 10b. Despite the control signal being saturated, the system still converges to the equilibrium point.

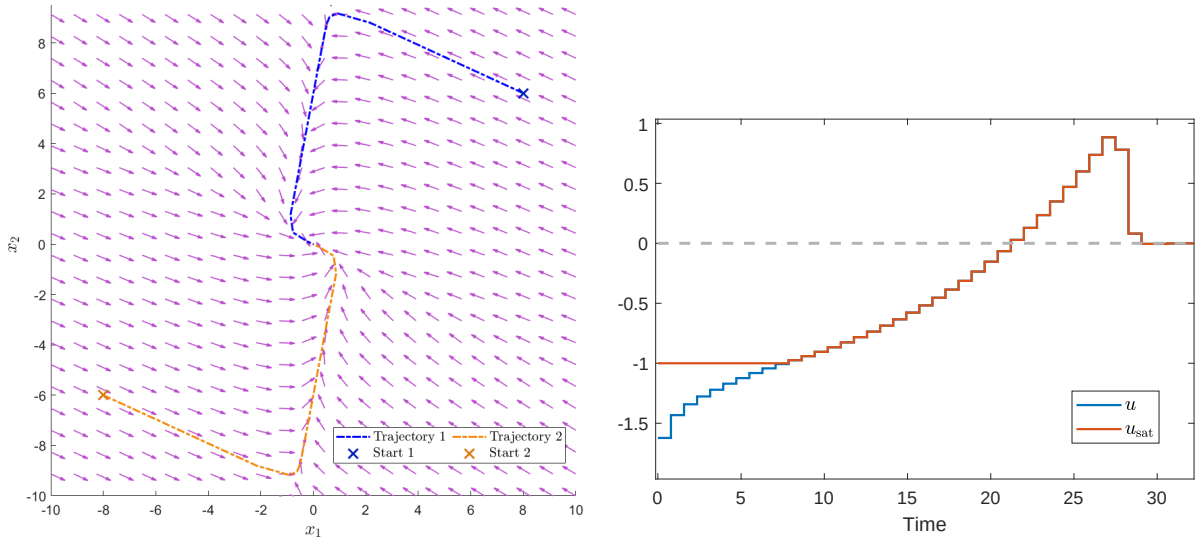

(a) Phase plane

(b) Control signal for trajectory 1

Figure 10: Trajectory convergence.

4.2 Regional Results

4.2.1 Regional Analysis

Theorem 3: Regional Analysis

Given any positive scalar $\tau > 0$, if there exist matrices $P_0 \in \mathbb{S}^n_{\succ 0}$, $P_1 \in \mathbb{R}^{n\times m}$, $P_2 \in \mathbb{S}^m$, $T_1 = \text{diag}(t_1, \ldots, t_m)$, $T_2 \in \mathbb{D}^n_{\succ 0}$, $T_3 \in \mathbb{D}^n_{\succeq 0}$, $Z_1 \in \mathbb{R}^{m\times n}$, and $Z_2 \in \mathbb{R}^{m\times m}$ satisfying conditions (28) and (30), with Z_1 and Z_2 defined as in (31), then the origin of system (11) is RAS.

For simplification purposes, we replace ru_0^2 with τt_i, which requires the following condition:

$$T_1 > \tau I_m$$

Optimization

To **maximize the region of stability**, one may include the additional condition (39), assuming:

$$\hat{P} \in \mathbb{S}^n_{\succ 0}, \quad \hat{T} \in \mathbb{D}^m_{\succ 0}$$

The optimization problem then becomes:

$$\min_{\substack{\hat{P},P_0,P_1,P_2,\\ \hat{T},T_1,T_2,T_3,Z_1,Z_2}} \text{Tr}(\hat{P})$$

Example 3) Based on the case study presented in [1], the continuous-time system (45) is described by the matrices

$$A_c = \begin{bmatrix} 0 & 1 \\ 1 & 0 \end{bmatrix}; \quad B_c = \begin{bmatrix} 0 \\ -5 \end{bmatrix}; \quad T_s = 0.4s; \tag{43}$$

Using the regional synthesis procedure, the following controller gains are obtained:

$$K_1 = \begin{bmatrix} -0.0186 & -1.3995 \end{bmatrix}; \qquad K_2 = 0.9963$$

This results in a Lyapunov matrix that is not positive definite, with P_2 being negative definite and P_0 positive definite, confirming a greater relaxation of the Lyapunov conditions, as shown below:

$$P = \begin{bmatrix} 0.0127 & 0.0235 & -0.0188 \\ 0.0235 & 1.3177 & -1.5390 \\ -0.0188 & -1.5390 & -3.7050 \end{bmatrix}$$

The phase portraits make it possible to observe the different behaviors of the system states with respect to their initial conditions. As predicted by the theory, all points inside the black ellipse $W(x)$ ensure convergence and are contained within the region where the sector condition is satisfied.

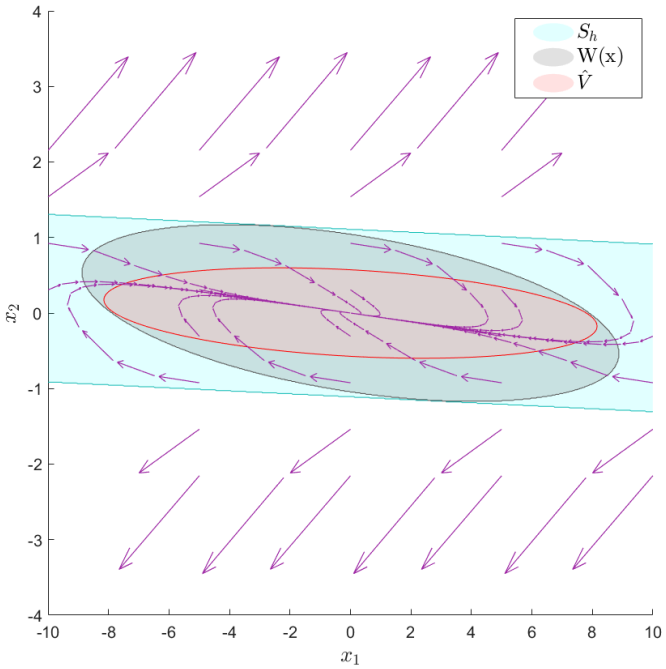

Figure 11: Phase plane: trajectory convergence.

Some points in Fig. 11, although converging to the origin, are not contained within the black region. This occurs because, although our proposed sign-indefinite Lyapunov structure is less conservative than the standard quadratic approach, the result still exhibits a certain degree of conservatism. In addition, the controller used in the analysis imposed a minimum convergence rate for the linear system through pole placement (optimization presented in Section 3.5.1). As a result, even though these trajectories converge, they may

not satisfy the minimum convergence rate requirement and are therefore not included in the set $W(x)$.

As shown in Fig. 12, the use of the sector condition makes it possible to determine a region of convergence even when the Lyapunov function takes negative values outside $\mathcal{S}_h$. This confirms the flexibility of the proposed model.

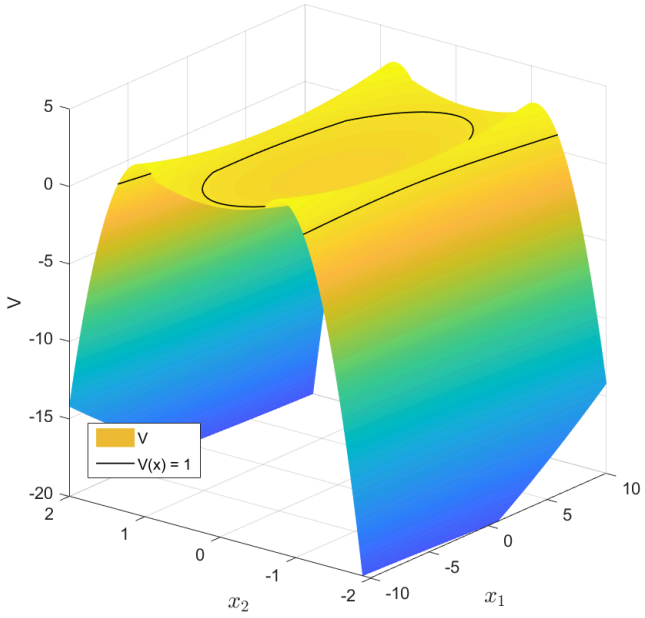

Figure 12: Lyapunov function negative outside $\mathcal{S}_h$ for the system in (44).

Example 4) Taken from [1], the continuous-time system is given by

$$A_c = \begin{bmatrix} 0 & 1 \\ 0 & 1 \end{bmatrix}; \qquad B_c = \begin{bmatrix} -1 \\ 1 \end{bmatrix}, \quad T_s = 0.8s. \tag{44}$$

Using the synthesis procedure, the following controller gains were obtained:

- $K_1 = \begin{bmatrix} 0.4734 & 0.4072 \end{bmatrix}$
- $K_2 = 0.9996$

It is possible to plot the system's region of convergence together with the limits of the sector condition S_h, as shown in Fig. 13. Furthermore, Fig. 14 shows that, even with control signal saturation, the system still converges to the equilibrium point.

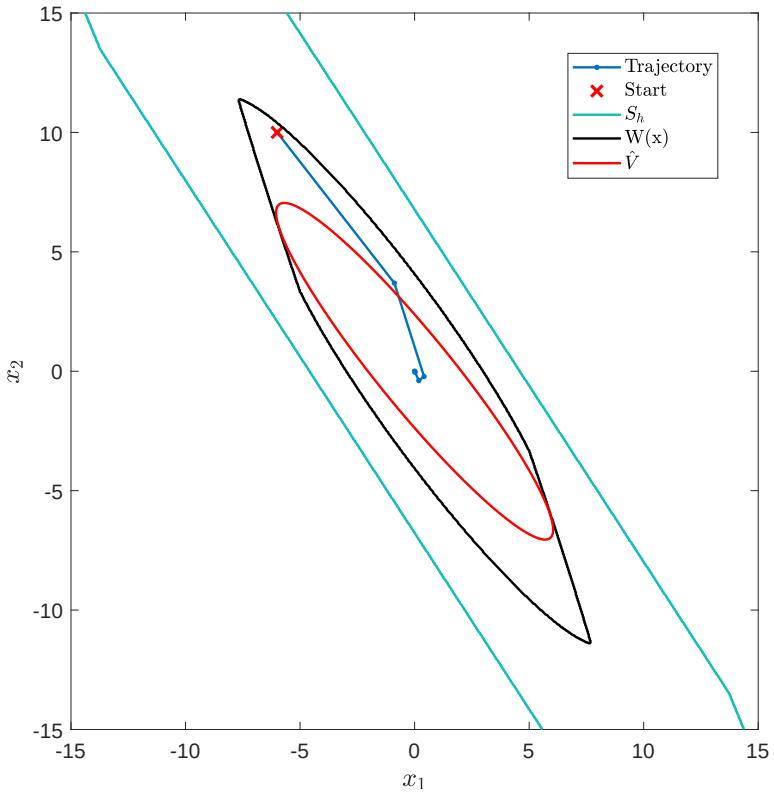

Figure 13: State trajectories for the system in (43).

It is worth noting that the solution obtained for the region $W(x)$, which guarantees asymptotic stability, does not touch the boundary of the sector condition. This indicates the possibility of improving the result, which can be achieved by modifying the minimization function to focus on directional optimization.

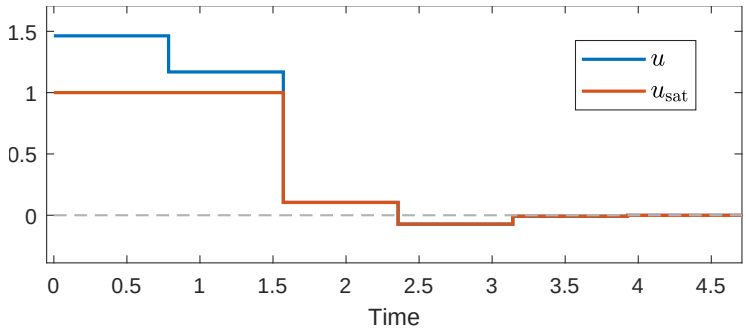

Figure 14: Control signal along the trajectories in Fig. 13 for $r = 0.2$.

4.2.2 Regional Synthesis

Theorem 4: Regional Synthesis

Given any positive scalar $r > 0$, if there exist matrices $Q_0 \in \mathbb{S}^n_{\succ 0}$, $Q_1 \in \mathbb{R}^{n\times m}$, $Q_2 \in \mathbb{S}^m$, $S \in \mathbb{D}^n_{\succ 0}$, $M \in \mathbb{R}^{n\times n}$, $Z_1 \in \mathbb{R}^{m\times n}$, $Z_2 \in \mathbb{R}^{m\times m}$, $Y_1 \in \mathbb{R}^{m\times n}$ and $Y_2 \in \mathbb{R}^{m\times m}$ that satisfy conditions (34) and (35), with Y_1, Y_2, Z_1 and Z_2 defined as in (32), and Q_0, Q_1, and Q_2 defined as in (33), then the origin of system (11) is RAS.

Optimization

To increase the **decay rate** of the system in the absence of saturation, one may include the additional condition (36), assuming $r \in [0, 1]$ and $R \in \mathbb{S}^n_{\succ 0}$.

To **maximize the region of stability**, one may include the additional condition (40), assuming $\hat{P} \in \mathbb{S}^n_{\succ 0}$.

The optimization problem then becomes:

$$\min_{\substack{R,\hat{P},Q_0,Q_1,Q_2,\\ M,S,Y_1,Y_2,Z_1,Z_2}} \operatorname{Tr}(\hat{P})$$

Returning to **Example** (44), the previously computed controller corresponds to the region shown in Fig. 15, with the associated control signal presented in Fig. 16.

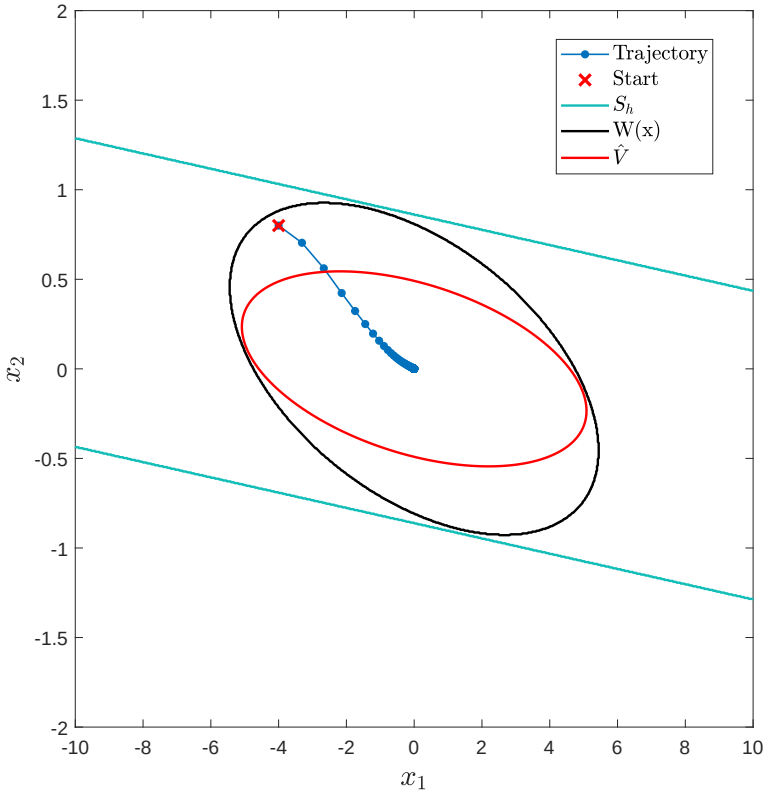

Figure 15: Trajetoria de estados sistema (44)

Note that the region in Fig. 15 is smaller than that in Fig. 11 (see scale of the plots) because, as discussed in Section 3.4, the synthesis formulation enforces the use of identical matrices T_1, T_2, T_3, and $\hat{T}$, which increases conservatism. In contrast, during the analysis phase, these matrices are allowed to take different values, resulting in a less conservative and potentially larger estimated region.

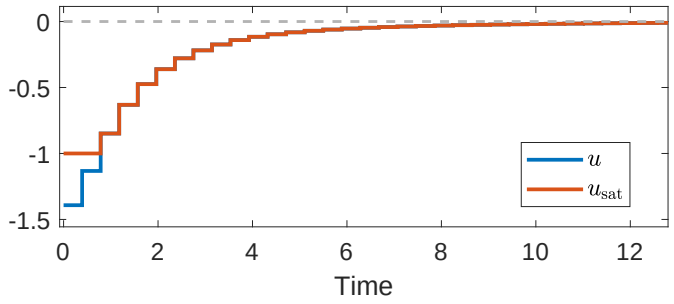

Figure 16: Control signal along the trajectories in Fig. 15 for $r = 0.95$.

Returning to **Example** (43), reducing the radius can be beneficial for increasing the system's speed in the absence of saturation. However, it also reduces the basin of stability, as seen in Fig. 11, where some points still ensure stability but lie outside the region $W(x)$ because they do not meet the minimum convergence rate requirement.

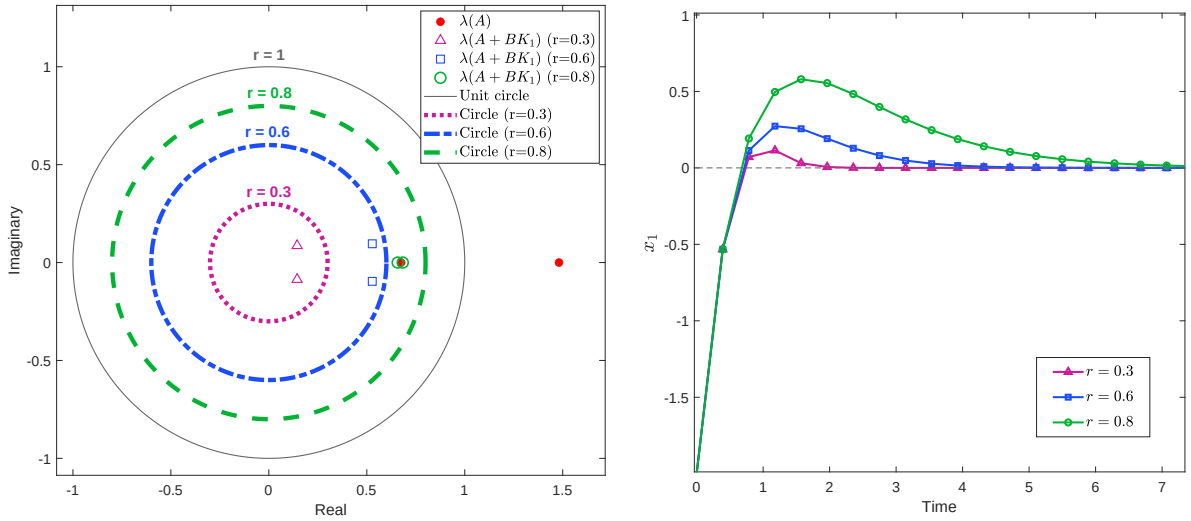

(a) Pole placement.

(b) State convergence.

Figure 17: Results for different decay rates r.

5 Conclusion

This work presented the discrete-time implementation of the analysis and synthesis methods proposed in [1] for systems subject to input saturation. The study addressed both global and regional approaches, building upon the theoretical framework of sector conditions and Lyapunov stability, including cases where the Lyapunov matrix is not necessarily positive definite. The entire implementation was carried out in MATLAB with a modular structure, and the developed codes were made available in [14] to facilitate reproducibility and future extensions.

In the global synthesis, the computed controllers ensured stability and allowed pole placement to accelerate the convergence rate within the linear region.

In the regional synthesis, the estimated regions of attraction closely matched the theoretical predictions. The results also revealed a clear trade-off between increasing speed and reducing the basin of stability. Notably, it was demonstrated that the proposed LMI formulations can still guarantee stability even when the Lyapunov function takes negative values outside $\mathcal{S}_h$, confirming the flexibility of the approach.

Overall, the discrete-time replication successfully reproduced the main results reported in the continuous-time formulation, while providing a clear and reproducible framework suitable for practical application.

Future work can focus on testing the methodology with a wider range of plant models, exploring different system dimensions, operating conditions and performing experimental validation. In some cases solver parameter settings resulted in infeasibility or produced overly narrow convergence regions due to poor variable scaling. For this reason additional efforts should be devoted to improving numerical conditioning and tuning with the aim of enhancing computational efficiency and scalability for larger and more complex problems.

List of Figures

A List of Annexes

A.1 Discretization

In state-space form, a continuous-time linear system is typically described as:

$$\begin{cases} \dot{x}(t) = A_c\, x(t) + B_c\, u(t), \\ y(t) = C\, x(t) + D\, u(t), \end{cases} \tag{45}$$

where $x(t)$ is the state vector, $u(t)$ is the input vector, and $y(t)$ is the output vector.

Choosing an appropriate sampling period T_s is essential to ensure that the discrete-time model accurately reproduces the dynamics of its continuous counterpart and to prevent aliasing. In Fig. 18 from [17], the impacts of aliasing on aircraft motion detection can be observed.

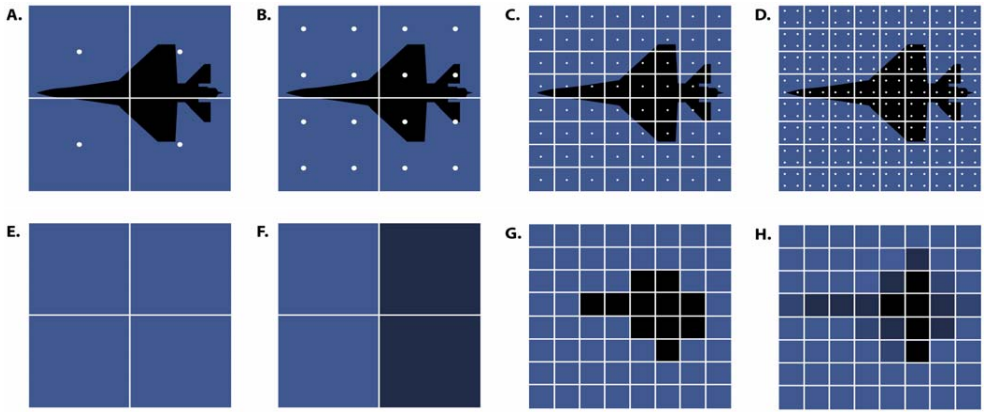

Figure 18: Example of aliasing in motion detection. Source: [17]

The Bode diagram of the continuous-time model can be used to determine the highest relevant frequency for sampling, based on the system bandwidth. The bandwidth ω_{BW} is defined as the frequency at which the gain drops by 3 dB from the low-frequency plateau, or at the resonance peak if one is present. This value represents the fastest significant dynamics to be preserved in the discrete-time model.

According to the Nyquist–Shannon sampling theorem, the maximum admissible sampling period without aliasing is given by:

$$T_{s_{\max}} = \frac{1}{f_{s_{\max}}} = \frac{1}{2 f_{BW}}, \quad f_{BW} = \frac{\omega_{BW}}{2\pi}$$

Choosing $T_s > T_{s_{\max}}$ places the sampling frequency beyond the range where the system exhibits significant gain. In this high-frequency region, the plant's natural attenuation effectively suppresses residual components, so that any aliased content has negligible influence on the accuracy of the discrete-time model.

By sampling the system, the equivalent discrete-time model is obtained as (1), where A and B are computed from (A_c, B_c) using a discretization method, such as the matrix exponential for a zero-order hold.

In this work, whenever continuous-time examples are presented, the system will be assumed linear, and the saturation nonlinearity will be incorporated only after discretization.

It is important to highlight that the examples presented in 4 contain all frequency components and, in practice, are not strictly band-limited, as illustrated in the Bode diagram of Fig. 19. In such systems, although the magnitude decreases continuously, it never vanishes. Consequently, regardless of the chosen sampling period, some residual aliasing effect will always remain. A common approach is to apply an anti-aliasing filter prior to discretization. Here, however, for simplicity, we will assume the signal to be band-limited.

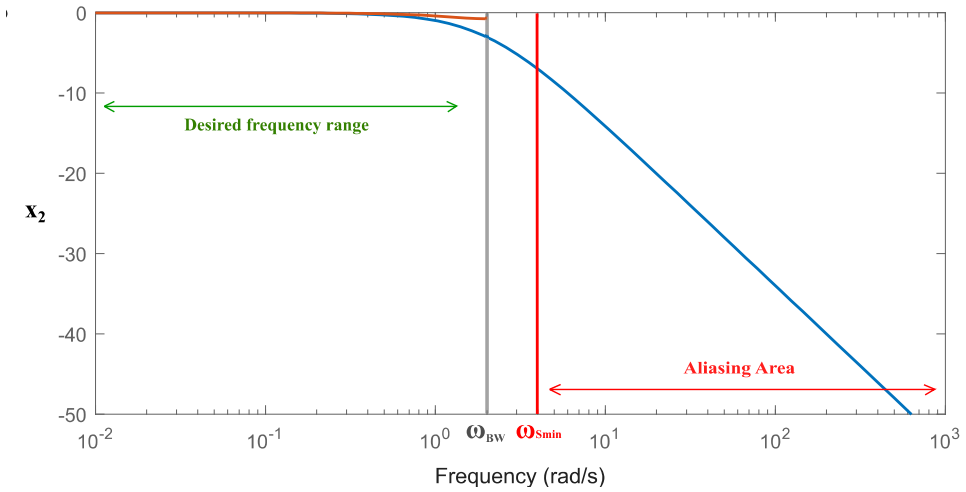

Figure 19: Bode diagram. ω_{BW} indicates the angular bandwidth frequency ($-3\,\mathrm{dB}$), and ω_A denotes the angular aliasing frequency. The *desired frequency range* contains the relevant signal content, while the *aliasing area* represents the region whose effect can be neglected in the discretization process.

The sampling time was chosen according to the criteria Nyquist. As shown in Fig. 19, the sampling frequency must be sufficiently higher than the system's bandwidth to ensure that the discrete-time model accurately reproduces the dynamics of the continuous-time system. This choice prevents significant distortion of the magnitude response at higher frequencies and preserves the essential dynamics in the discretized model.

A.2 Well-Posedness

A system is said to be well-posed if it satisfies the following three conditions:

1. A solution exists;
2. The solution is unique;
3. The solution depends continuously on the input data.

These requirements ensure that the system's behavior is mathematically consistent and predictable. In the context of this work, well-posedness is essential because, once the control law is defined, it guarantees that there is a unique system trajectory corresponding to each initial condition. This avoids ambiguous behaviors or potential instabilities that could arise from multiple admissible control responses for the same state.

A.3 Interpretation of the Sector Condition

In control theory, the sector condition specifies a subset S_h of the state space where a given property is satisfied. Instead of requiring a property to hold everywhere, it is enough that it holds inside S_h, which often allows the stability analysis to be less conservative.

Consider a system variable ν subject to a nonlinearity function $\psi(\nu)$. This nonlinearity can, without loss of generality, be represented as in Fig. 20, where the lines with slopes α and β delimit the blue region S_h in the state space.

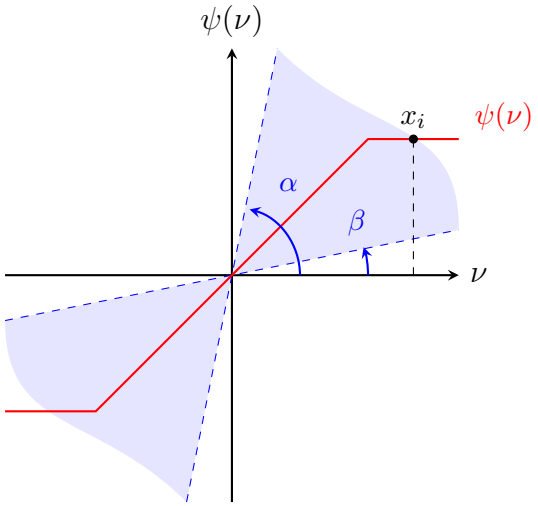

Figure 20: Representation of a nonlinear function within a sector S_h.

Thus, for any $x_i \geq 0$ within S_h, the function $\psi(\nu)$ satisfies:

$$\tan(\beta)\, x_i \leq \psi(x_i) \leq \tan(\alpha)\, x_i.$$

Equivalently, this can be expressed as:

$$0 \leq \psi(x_i) - x_i \tan(\beta) \quad \text{and} \quad \psi(x_i) - x_i \tan(\alpha) \leq 0,$$

Since the product of these two terms is always non-positive, the sector condition can be written as:

$$(\psi(x_i) - x_i \tan(\alpha))^\top T(\psi(x_i) - x_i \tan(\beta)) \leq 0, \tag{46}$$

where T is a positive diagonal matrix used to ensure dimensional compatibility in multi-variable cases. This condition also holds for $x_i < 0$.

In this work, ψ corresponds to the saturation function applied to the control signal u. In the global case, $\alpha = 45°$ and $\beta = 0$, giving:

$$(sat(u) - u)^\top T\,(\text{sat}(u)) \geq 0 \tag{47}$$

which, using the dead-zone definition in (7), this relation becomes equivalent to (16). For all points defined by the saturation function, the sector condition is valid, corresponding to the global case (see Fig. 21a).

For the regional sector condition, a function $h(x)$ defined in (13) is introduced to act as a lower bound for the region (see Fig. 21b). In this case, the new regional sector condition can be expressed as:

$$(sat(u) - u)^\top T \left(\text{sat}(u) - h(x)\right) \geq 0 \tag{48}$$

which is equivalent to (17).

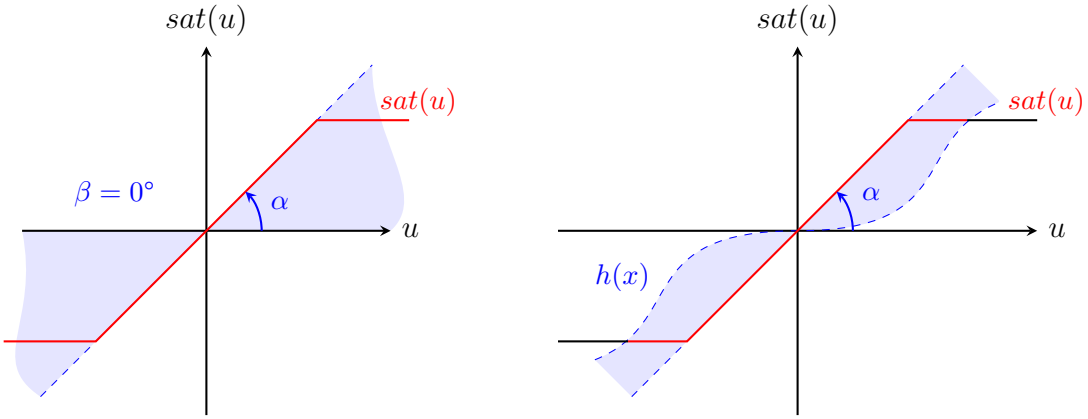

(a) Global. (b) Regional.

Figure 21: Sector condition.

A.4 Dead-Zone Signal Property

This subsection analyzes the properties in (16) and (18) based on the sign variation of the dead-zone function.

The goal is to determine, for each possible transition of the signal, the sign of the dead-zone variation and the corresponding saturation variation.

The dead-zone function $dz(u_i)$ can be divided into three operating regions:

(+) Positive values: when u_i exceeds the upper saturation limit;

(0) Zero values: when u_i lies within the saturation limits;

(−) Negative values: when u_i is below the lower saturation limit.

$$dz(u_i) = \begin{cases} u_i - 1, & \text{si } 1 \leq u_i; \quad (+) \\ 0, & \text{si } -1 \leq u_i \leq 1; \quad (0) \\ u_i + 1, & \text{si } u_i \leq -1. \quad (-) \end{cases} \tag{49}$$

This reasoning can be extended to the variation of the saturation signal. From (7), we obtain:

$$\Delta sat = u_i^+ - u_i - \Delta dz$$

By systematically evaluating all combinations of initial and future states, we can determine the variations of both the dead-zone signal and the saturation signal. For instance, subtracting a negative value from a positive one will always yield a positive result. The complete set of cases is summarized in Table 2.

A key observation is that the sign of the product between these variations is always known: even in cases where the sign of one function is uncertain (denoted by the symbol (**?**)), the other is zero, making the product zero as well.

dz^+	dz	Δdz		Δsat	
$+$	$+$	$u_i^+ - u_i$	?	0	0
$+$	0	$u_i^+ - 1$	$+$	$-(u_i - 1)$	$+$
$+$	$-$	$u_i^+ - u_i - 2$	$+$	2	$+$
0	$+$	$-(u_i - 1)$	$-$	$u_i^+ - 1$	$-$
0	0	0	0	$u_i^+ - u_i$	?
0	$-$	$-(u_i + 1)$	$+$	$u_i^+ + 1$	$+$
$-$	$+$	$u_i^+ - u_i + 2$	$-$	-2	$-$
$-$	0	$u_i^+ + 1$	$-$	$-(u_i + 1)$	$-$
$-$	$-$	$u_i^+ - u_i$	?	0	0

Table 2: Sign variation analysis for the saturation function.

A.5 Convex Reformulation – Synthesis

The purpose of this section is to present the derivation behind the expansion of the stability condition for the Lyapunov variation, from (30) to (35).

The same procedure will be applied to (40), starting from the expansion of (39).

Expansion of the Lyapunov Condition

For the derivation, the regional form of the sector condition (48) will be used. As a special case, when dealing with global stability, it is sufficient to set $H_1 = 0$ and $H_2 = 0$. The same simplification applies to Z_1 and Z_2, as described in Section 3.4.

We begin by rewriting matrices (29) and (18) in the expanded basis including x^+, obtaining, respectively:

$$\begin{bmatrix} x \\ dz \\ x^+ \\ dz^+ \end{bmatrix}^\top \begin{bmatrix} -P_0 & -P_1 & 0 & 0 \\ -P_1^\top & -P_2 & 0 & 0 \\ 0 & 0 & P_0 & P_1 \\ 0 & 0 & P_1^\top & P_2 \end{bmatrix} \begin{bmatrix} x \\ dz \\ x^+ \\ dz^+ \end{bmatrix} \tag{50}$$

$$\begin{bmatrix} x \\ dz \\ x^+ \\ dz^+ \end{bmatrix}^\top \begin{bmatrix} 0 & 0 & 0 & 0 \\ S^{-1}K_1 & S^{-1}(K_2 - I_m) & -S^{-1}K_1 & -S^{-1}(K_2 - I_m) \\ 0 & 0 & 0 & 0 \\ -S^{-1}K_1 & -S^{-1}(K_2 - I_m) & S^{-1}K_1 & S^{-1}(K_2 - I_m) \end{bmatrix} \begin{bmatrix} x \\ dz \\ x^+ \\ dz^+ \end{bmatrix} \tag{51}$$

As observed, the expansion related to (18) already introduces the variable substitution that will be applied throughout the formulation, namely $T_2 = T_3 = S^{-1}$. In addition, the

reader is encouraged to visualize the expansion of (18) based on the definitions (9), (7), and (13).

Moreover, from (11), we can derive the following expression:

$$\eta^\top N \left[-x^+ + (A + BK_1)x + B(K_2 - I_m)dz\right] = 0 \tag{52}$$

where $\eta = \begin{bmatrix} x; & dz; & x^+; & dz^+ \end{bmatrix}$ is the expanded state vector, and $N = \begin{bmatrix} 0 & 0 & M^{-1} & 0 \end{bmatrix}^\top$ is an auxiliary matrix introduced to facilitate the convex reformulation of the system.

Thus, (52) can be rewritten in matrix form as:

$$\begin{bmatrix} x \\ dz \\ x^+ \\ dz^+ \end{bmatrix}^\top \begin{bmatrix} 0 & 0 & 0 & 0 \\ 0 & 0 & 0 & 0 \\ M^{-\top}(A + BK_1) & M^{-\top}B(K_2 - I_m) & -M^{-\top} & 0 \\ 0 & 0 & 0 & 0 \end{bmatrix} \begin{bmatrix} x \\ dz \\ x^+ \\ dz^+ \end{bmatrix} = 0 \tag{53}$$

By combining matrices (17), (50), (51), and (53), and then post and pre-multiplying by $\text{diag}(M, S, M, S)$ and its transpose, respectively, it is possible to obtain matrix (35) through the substitution of the convex reformulation variables (32) and (33).

Expansion of the Optimization Condition

The expansion of the optimization condition for $\hat{V}$, previously presented in (39), also applies the reformulation using the matrix $S^{-1} = T$.

By post- and pre-multiplying by the matrix $\text{diag}(M, S)$ and its transpose, respectively, we obtain:

$$\begin{bmatrix} M^\top \hat{P} M - Q_0 & * \\ -Q_1^\top - Y_1 + Z_1 & -Q_2 - \text{He}(Y_2 - S - Z_2) \end{bmatrix} \succ 0 \tag{54}$$

From the property given in (37), we can deduce that:

$$\begin{bmatrix} M^\top + M - \hat{P} - Q_0 & * \\ -Q_1^\top - Y_1 + Z_1 & -Q_2 - \text{He}(Y_2 - S - Z_2) \end{bmatrix} < \begin{bmatrix} M^\top \hat{P} M - Q_0 & * \\ -Q_1^\top - Y_1 + Z_1 & -Q_2 - \text{He}(Y_2 - S - Z_2) \end{bmatrix} \tag{55}$$

Since $\hat{P}$ is positive definite, matrix (55) can be rewritten to make the Schur complement explicitly visible:

$$\begin{cases} \hat{P} \succ 0 \\ \begin{bmatrix} M^\top + M - Q_0 & * \\ -Q_1^\top - Y_1 + Z_1 & -Q_2 - \text{He}(Y_2 - S - Z_2) \end{bmatrix} - \begin{bmatrix} I_n \\ 0 \end{bmatrix} \hat{P}^{-1} \begin{bmatrix} I_n & 0 \end{bmatrix} \succ 0 \end{cases}$$

Recalling that if a matrix is positive definite, its inverse is also positive definite, the Schur complement leads to:

$$\begin{bmatrix} M^\top + M - Q_0 & * & * \\ -Q_1^\top - Y_1 + Z_1 & -Q_2 - \mathrm{He}(Y_2 - S - Z_2) & * \\ I_n & 0 & \hat{P} \end{bmatrix} \succ 0$$

which is equivalent to the matrix given in (40):

$$\begin{bmatrix} M^\top + M - Q_0 & * & * \\ I_n & \hat{P} & * \\ -Q_1^\top - Y_1 + Z_1 & 0 & -Q_2 - \mathrm{He}(Y_2 - S - Z_2) \end{bmatrix} \succ 0$$

References

[1] Isabelle Queinnec et al. "Design of Saturating State Feedback With Sign-Indefinite Quadratic Forms". In: *IEEE Transactions on Automatic Control* PP (Aug. 2021), pp. 1–1. DOI: 10.1109/TAC.2021.3106878.

[2] Sergio Galeani et al. "A Tutorial on Modern Anti-windup Design". In: *European Journal of Control* 15.3 (2009), pp. 418–440. ISSN: 0947-3580. DOI: https://doi.org/10.3166/ejc.15.418-440. URL: https://www.sciencedirect.com/science/article/pii/S0947358009709987.

[3] Sophie Tarbouriech and Isabelle Queinnec. "Un tour d'horizon sur les techniques anti-windup pour les systèmes saturés". In: *Techniques de l'Ingénieur* (2020). Disponible via HAL: https://laas.hal.science/hal-03070178.

[4] Pietro Ghignoni et al. "Anti-Windup Design for Directionality Compensation With Application to Quadrotor UAVs". In: *IEEE Control Systems Letters* 5.1 (2021), pp. 331–336. DOI: 10.1109/LCSYS.2020.3001881.

[5] Oleg I. Borisov et al. "Output robust control with anti-windup compensation for robotic boat". In: (2016), pp. 13–18. DOI: 10.1109/MMAR.2016.7575080.

[6] Maurice Filo, Ankit Gupta, and Mustafa Khammash. "Anti-Windup Protection Circuits for Biomolecular Integral Controllers". In: *bioRxiv* (2023). DOI: 10.1101/2023.10.06.561168. eprint: https://www.biorxiv.org/content/early/2023/10/19/2023.10.06.561168.full.pdf. URL: https://www.biorxiv.org/content/early/2023/10/19/2023.10.06.561168.

[7] Hassan K Khalil. *Nonlinear systems*. English. Upper Saddle River, N.J.: Prentice Hall, 2002. ISBN: 0130673897 9780130673893 0131227408 9780131227408.

[8] Sophie Tarbouriech et al. "Stability and Stabilization of Linear Systems With Saturating Actuators". In: Jan. 2011, pp. 51–121. ISBN: 978-0-85729-940-6. DOI: 10.1007/978-0-85729-941-3_2.

[9] João Jr, Romeu Reginatto, and Sophie Tarbouriech. "Anti-windup design with guaranteed regions of stability for discrete-time linear systems with saturating controls". In: *Controle and Automacao* 15 (Mar. 2004). DOI: 10.1590/S0103-17592004000100002.

[10] Philipp Braun et al. "Optimizing Shifted Stabilizers With Asymmetric Input Saturation". In: *IEEE Transactions on Automatic Control* 70.2 (2025), pp. 751–766. DOI: 10.1109/TAC.2024.3436728.

[11] Lixia Yan, Baoli Ma, and Yingmin Jia. "Trajectory tracking control of nonholonomic wheeled mobile robots using only measurements for position and velocity". In: *Automatica* 159 (2024), p. 111374. ISSN: 0005-1098. DOI: https://doi.org/10.1016/j.automatica.2023.111374. URL: https://www.sciencedirect.com/science/article/pii/S000510982300540X.

[12] Stephen Boyd and Lieven Vandenberghe. *Convex Optimization*. Cambridge University Press, 2004. ISBN: 9780521833783. URL: https://web.stanford.edu/~boyd/cvxbook/.

[13] Qiao Zhu, Guang-Da Hu, and Li Zeng. "Estimating the spectral radius of a real matrix by discrete Lyapunov equation". In: *Journal of Difference Equations and Applications* 17 (Apr. 2011), pp. 603–611. DOI: 10.1080/10236190903305443.

[14] Luana Albuquerque de Oliveira. *Sign-Indefinite Lyapunov - Internship Code Repository.*
`https://github.com/lu3705/Sign_Indefinite_Lyapunov.git`. 2025.

[15] Iswanto Suwarno et al. "Controllability and Observability Analysis of DC Motor System and a Design of FLC-Based Speed Control Algorithm". In: *Journal of Robotics and Control (JRC)* 3 (Feb. 2022), pp. 227–235. DOI: `10.18196/jrc.v3i2.10741`.

[16] Bahador Rashidi, Milad Esmaeilpour, and Mohammad Reza Homaeinezhad. "Precise angular speed control of permanent magnet DC motors in presence of high modeling uncertainties via sliding mode observer-based model reference adaptive algorithm". In: *Mechatronics* 28 (2015), pp. 79–95. ISSN: 0957-4158. DOI: `https://doi.org/10.1016/j.mechatronics.2015.04.009`. URL: `https://www.sciencedirect.com/science/article/pii/S0957415815000549`.

[17] Christine Covas, Julie Lindholm, and Craig Eidman. "P-28: Effect of Image Generation Variables on Aircraft-Roll Detection Range". In: *Sid Symposium Digest of Technical Papers* 37 (June 2006), p. 5. DOI: `10.1889/1.2433483`.

Code available at [14]:

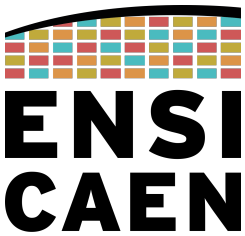

"Success springs from the will to achieve, the determination to persist, and the courage to face obstacles. Even without hitting the mark, those who strive will accomplish admirable feats"
- José de Alencar

Ecole Publique d'Ingénieurs en 3 ans

6 Boulevard Maréchal Juin
14000 Caen, France
https://www.ensicaen.fr